Cold Spray for Mitigation and Repair of Spent Nuclear Fuel Dry Storage Canisters

Spent Fuel and Waste Disposition

Prepared for
US Department of Energy

Spent Fuel and Waste
Science and Technology

K.A. Ross, P. Mayur, B. Gwalani
Pacific Northwest National Laboratory

T.J. Montoya, E. Karasz, R.F. Schaller
Sandia National Laboratories

September 30, 2021
M3SF-21PN010207032
PNNL-

SUMMARY

The purpose of this work is to investigate the use of cold spray for repair and mitigation of chloride-induced stress corrosion cracking (CISCC) in dry cask storage system (DCSS) canisters to ensure their integrity far beyond their original license period. This report provides a viability analysis of cold spray for repair and mitigation of CISCC in DCSS canisters to extend canister life.

Literature reports that the following three conditions must exist for CISCC to occur: tensile stress, a corrosive environment, and susceptible material. These conditions must be understood and accounted for while evaluating CISCC susceptibility. Furthermore, non-obvious factors, such as surface conditions and geometric confinement, can dramatically increase the intensity of one or more of the three listed conditions for CISCC.

It is known that areas in and around fusion welds in alloys used for spent nuclear fuel storage canisters have increased CISCC susceptibility relative to the base metal. Cold spray has the potential to extend the life of DCSS canisters by coating damaged or susceptible areas with cold spray corrosion barriers and inducing beneficial compressive residual stresses.

Cold spray should be considered for manufacturing, CISCC mitigation, and repair of canisters. Cold spray has demonstrated the ability to deposit stainless steel (SS), Inconel alloys, and other alloys on SS 304L. The technical basis for cold spray application within the overpack using remote robotic equipment is established. A non-obvious application to the research community is the sealing of crevices. All instances of CISCC in the field, for nuclear applications, reported by the Pressurized Water Reactor Owners Group were associated with crevice corrosion. This can be avoided by cold spraying to seal crevices.

A significant amount of work needs to be done to develop cold spray for DCSS canister repair and mitigation. Coating powder chemistries need to be selected such that no detrimental galvanic effects occur and CISCC resistance is maximized. Identifying the optimal chemistry for canister protection is an area that demands a significant R&D effort.

Surface roughness/texture effects are expected to affect CISCC initiation. Cold spray parameters and powder preparation can affect surface roughness. Testing should be done to develop an understanding of how surface roughness/texture developed by cold spray affects CISCC initiation.

This project performed preparatory work and is in the process of generating cold spray samples for CISCC testing by collaborative projects at Pacific Northwest National Laboratory and Sandia National Laboratories. This task will identify the effect of process parameters on microstructure and CISCC resistance. Optimized parameters will be used to produce a smaller number of coupons for full testing and evaluation.

This report presents an analysis of cold spray for canister life extension, a summary of related efforts, relevant technology down selections, work accomplished to date, and future work relative to the use of cold spray for repair and mitigation of CISCC in DCSS canisters. This work presents experimental work including mechanical and corrosion testing results for various cold sprayed materials and parameters. Initial results indicate the interface between the cold sprayed material and the substrate needs to be further studied to understand

This page is intentionally left blank

ACKNOWLEDGMENTS

The authors would like to express their sincere thanks to the project's U.S. Department of Energy's sponsor, Ned Larson, for supporting and funding this work.

The authors would also like to thank our Sandia National Laboratories collaborators on this work.

This page is intentionally left blank

CONTENTS

LIST OF FIGURES

LIST OF TABLES

ACRONYMS

ANL	Argonne National Laboratory
APS	atmospheric plasma spraying
BRC	Blue Ribbon Commission on America's Nuclear Future
BWR	boiling water reactor
CAPS	controlled atmosphere plasma spraying
CISCC	chloride-induced stress corrosion cracking
CTE	coefficients of thermal expansion
COVID-19	Coronavirus disease 2019
CNC	Computer Numerical Control
CP	Commercially Pure
CPVC	chlorinated polyvinyl chloride
CSC	cesium and strontium capsule
DCPD	direct current potential drop
DCS	dry cask storage
DCSS	dry cask storage system
DoD	U.S. Department of Defense
DOE	U.S. Department of Energy
DPC	dual-purpose canister
DST	double-shell tank
EM	(Office of) Environmental Management
EPRI	Electric Power Research Institute
ESCP	Extended Storage Collaboration Program
FEA	finite element analysis
FY	fiscal year
HAZ	heat-affected zone
HPCS	high-pressure cold spray
HPPS	high-pressure plasma spraying
ISFSI	Independent Spent Fuel Storage Installations
IGSCC	intergranular stress corrosion cracking
ISFSI	independent spent fuel storage installation
LPCS	low-pressure cold spray
LPPS	low-pressure plasma spraying
MCSC	Management of Cesium and Strontium Capsule
NDE	non-destructive evaluation
NRC	U.S. Nuclear Regulatory Commission
PNNL	Pacific Northwest National Laboratory
PVD	physical vapor deposition

SBIR	Small Business Innovation Research
SCC	stress corrosion cracking
SEM	scanning electron microscopy
SFWD	Spent Fuel and Waste Disposition
SNL	Sandia National Laboratories
SONGS	San Onofre Nuclear Generating Station
SPP	Solid Phase Processing
SSs	Stainless Steels
RT	Room Temperature
UWM	University of Wisconsin-Madison
VPS	vacuum plasma spraying

INVESTIGATION OF COLD SPRAY AS A DRY STORAGE CANISTER REPAIR AND MITIGATION TOOL

1 INTRODUCTION

The lack of a permanent spent nuclear fuel repository means utilities are faced with extending licenses for dry cask storage systems (DCSS) canisters far beyond their original 20-year license period. In fact, license extension has already been granted at selected sites for up to 40 years with an expectation of further extension of 40 years more (NRC 2012). DCSS canisters are typically made of austenitic stainless steel (SS) cylinders that are closed using fusion welds to provide leak-tight containment of the spent fuel. With extension beyond their designed service life, chloride-induced stress corrosion cracking (CISCC) has become a major concern to the long-term integrity of DCSS canisters, especially in the welded region. This is because many DCSS canisters are located near salt-water bodies or other sources of chlorides, where chloride (Cl)-rich deliquescent brines can deposit on canisters, creating a susceptible environment for CISCC precursor to form. In addition, high residual tensile stress and susceptible microstructure resulting from the high heat input and melting/subsequent cooling during the fusion welding process can provide susceptible mechanical and material conditions for CISCC initiation and propagation. The purpose of the work reported here is to investigate the use of cold spray for repair and mitigation of CISCC in DCSS canisters to ensure integrity far beyond their original license period.

This report presents an analysis of cold spray for canister life extension, a summary of related efforts, relevant technology down selections, work accomplished, and future efforts relative to the use of cold spray for repair and mitigation of CISCC in DCSS canisters.

1.1 Chloride-Induced Stress Corrosion Cracking

Three conditions must exist for CISCC to occur: tensile stress, a corrosive environment, and susceptible material (Figure 1). These conditions must be understood and accounted for when evaluating CISCC susceptibility. Furthermore, non-obvious factors, such as surface conditions and geometric confinement, can significantly affect the intensity of one or more of the three listed conditions for CISCC.

DCSS canisters are made from austenitic SSs that contain 16–18 weight percent of chromium (Cr) in the solid solution for enhanced resistance to corrosion. Arc welding is used at all confinement boundary closure locations. High heat input associated with arc welding melts material along the weld line. The molten material shrinks during solidification, thereby creating tensile residual stresses.

The region that melts between the joint line during fusion welding is called the fusion zone. The region adjacent to the fusion zone that does not melt but is affected by weld heat input is the heat-affected zone (HAZ). During fusion welding of austenitic SSs, high heat input causes Cr-rich carbides to precipitate along grain boundaries, leading to Cr depletion at grain boundaries. This Cr depletion at the grain boundaries is referred to as sensitization. Sensitization results susceptibility to intergranular (IG) corrosion. Intergranular corrosion accelerated by stresses in the material is called intergranular stress corrosion cracking (IGSCC). Stainless steels with low carbon content, denoted by “L,” were developed to mitigate sensitization during arc welding.

To provide a technical basis for extended storage capabilities, the U.S. Department of Energy (DOE) performed a gap analysis (Hanson et al. 2012) identifying that the DCS container welds fabricated using conventional fusion welding processes were sensitive to CISCC. Research work by Sandia National Laboratories (SNL) and others has shown that through-wall tensional residual stresses exist in current DCS containers. When combining these characteristics, canister performance over extended periods of time becomes less certain.

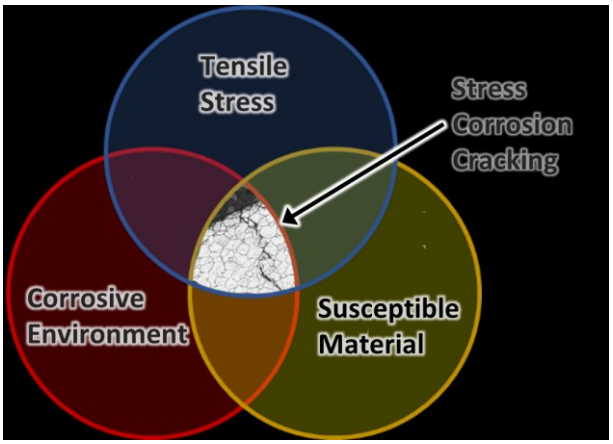

Figure 1. Three conditions required for SCC.

Cold spray is a potential solution to mitigate CISCC in DCSS canisters. During cold spray no melting occurs and the energy input can be controlled such that detrimental effects to the base metal during these processes are reduced and possibly eliminated. The goal of this work is to develop and demonstrate cold sprayed coatings with improved CISCC resistance relative to SS 304/304L base metal in and around the processed regions. Cold spray produces a corrosion barrier that separates the susceptible material from a corrosive environment. Furthermore, cold spray can induce compressive residual stresses in the coating and in the substrate material immediately beneath. Canister material directly beneath a cold spray coating is not exposed to the corrosive environment and is in a compressive residual stress condition and CISCC is mitigated.

1.2 Arc Welding

Arc welding uses an electric arc to join metal by melting materials at the interface. This has been a standard technology for joining metals for nearly a century. Currently, arc welding is the standard fabrication and repair technology for the nuclear and many other industries. The DOE (Hanson et al. 2012) and U.S. Nuclear Regulatory Commission (2012) determined residual stresses resulting from fusion welds in austenitic DCSS canisters put the fusion weld areas at higher risk for CISCC than for base metal.

1.2.1 Advantages

Arc welding is currently used for fabrication and repair of steel components for many applications. Some advantages of arc welding relative to canister repair are listed below.

- Manual and automated equipment are commercially available.
- Robotic solutions for repair within overpack are at a high technology readiness level.
- Relevant codes and code cases exist for various arc welding repair processes.

1.2.2 Technical Challenges

- Fundamental physics issues cause reduced CISCC resistance of material in and around arc welded zones.
- Weld shrinkage associated with resolidification produces residual tensile stress in and around the weld, making it susceptible to further degradation such as cracking.

- High heat input and melting, and subsequent cooling cause microstructural and microchemical changes in and around welds, making them more susceptible to corrosion and SCC.

Arc welding, shown in Figure 2, is considered for temporary and permanent repairs. It is known that alloys used in the existing inventory of spent nuclear fuel storage canisters have reduced CISCC resistance in areas around fusion welds. Ideally, fusion welding used for repair should be combined with a mitigation technique, such as cold spray coating on the weld and the HAZ.

Figure 2. Arc welding of a DCSS canister provided by Fluor.

This page is intentionally left blank

1.3 COLD SPRAY FOR CANISTER LIFE EXTENSION

Cold spray is a technology of interest for repair and mitigation of CISCC in DCSS canisters. Canister life in this report refers to extending canister life through CISCC repair and/or mitigation techniques. This section provides a summary of background information relative to cold spray technology relative to canister life extension. A comprehensive review of cold spray technology relative to canister life extension is included in last year's report (Ross et al. 2020). A comprehensive review of cold spray technology for nuclear applications is given in a recently published NRC report (Ross et al. 2021).

1.4 Process Description

Metal spray coating processes use heated gas to propel metal particles that bond to a substrate material. Thermal spray is a family of metal spray coating processes where particles are fully or partially melted during the process and re-solidified after impacting the substrate. Thermal spray processes include plasma spray, detonation spray, high-velocity oxy fuel spray, and their variants. Because melting and resolidification occur during thermal spray, tensile residual stresses are caused by the shrinking that takes place during resolidification. Oxidation and undesirable chemical reactions also occur due to high heat input and melting. Most thermal spray processes are limited in build thickness to 1 mm or less. In limited cases, build thickness can be somewhat thicker. Mechanical interlocking of solidified particles is the bonding mechanism for thermal spray.

Cold spray is a solid phase metal spray process during which no melting occurs. Metal particles are carried by a heated gas stream that softens the metal and propels particles at high velocities. The impact energy is high enough to bond metal particles to the surfaces they impact. Because it is a solid phase process, cold spray avoids oxidation, tensile residual stresses, and other detrimental effects typical of the high heat input and melting associated with thermal spray. Cold spray can produce infinitely thick coatings with beneficial compressive residual stresses.

Some researchers in the thermal spray community describe cold spray as a type of thermal spray. This is incorrect. Melted particles are part of the definition of thermal spray (TWI 2020; VRC 2020). The technical driver for cold spray development and commercialization was the avoidance of issues associated with high heat input, melting, and resolidification that occur during thermal spray processes. For the purpose of this report, cold spray refers to metal spray processes in which no melting occurs and thermal spray refers to metal spray processes in which melting occurs.

Cold spray can produce superior properties relative to thermal spray for materials of interest in spent nuclear fuel storage and transportation applications. Furthermore, oxidation and tensile residual stresses are attributes of thermal spray that impair properties and make the material more susceptible to CISCC. Therefore, thermal spray processes are low priority for evaluation for CISCC repair and mitigation.

High-pressure cold spray (HPCS) is the metal spray process of greatest interest for CISCC repair and mitigation. Figure 3 shows a diagram of HPCS where particles are accelerated to supersonic velocities and impact a substrate. Figure 4 shows nickel (Ni) deposited using HPCS. During the process, substrate heating is minimal, dimensional stability is maintained, and unwanted thermal effects (HAZ, thermal stresses, dilution layer formation, etc.) are avoided. HPCS systems operate at pressures typically ranging from 300 to 1,000 psi (VRC 2020) and typically produce particle velocities ranging from 800 to 1400 m/s (Moridi et al. 2014). High velocity enables high kinetic energy, which is required to create high plastic deformation and shearing at particle surfaces. This results in dynamic recrystallization and metallurgical bonding at interparticle boundaries. Particles are held to each other and to the substrate by both mechanical interlocking and metallurgical bonding.

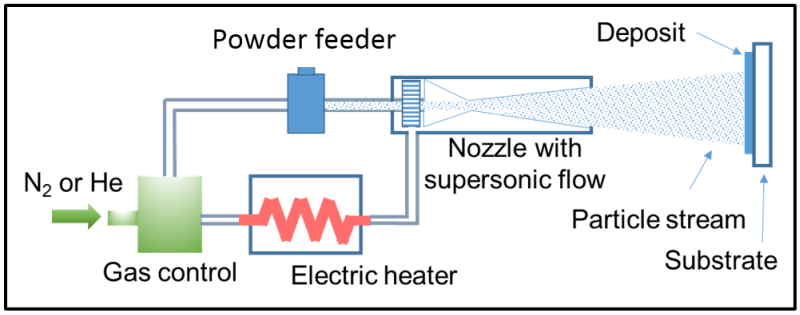

Figure 3. HPCS process diagram.

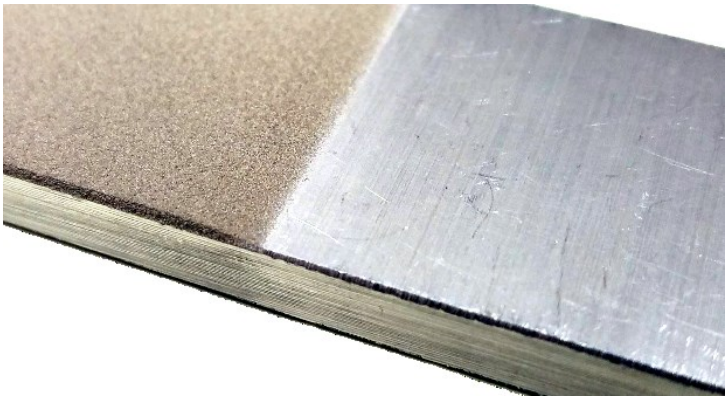

Figure 4. HPCS coating of commercially pure nickel sprayed (left side) at PNNL.

Low-pressure cold spray (LPCS) is of lesser interest because it fails to propel particles fast enough to achieve the kinetic energy needed for high-quality cold spray deposition of alloys with high melting temperatures. LPCS systems operate at 300 psi and lower (VRC 2020). They typically produce particle velocities ranging from 300 to 600 m/s (Moridi et al. 2014). Reduced kinetic energy associated with LPCS means less plastic deformation, less interlocking, and no or dramatically reduced metallurgical bonding in materials with high melting points. Reduced kinetic energy means deteriorated mechanical properties relative to HPCS. LPCS systems are not recommended for high-quality cold spray of steels, Inconel, and other high strength/melt temperature materials.

Kinetic metallization, pulsed gas dynamic spraying, vacuum cold spray, and warm spray are cold spray variants. These variants have not demonstrated the ability to match properties that can be achieved using HPCS for materials of interest for spent nuclear fuel canister repair and mitigation.

The rest of this section focuses on HPCS because it has advantages and improved properties compared to competing metal spray techniques.

1.5 Corrosion Protection Mechanism

Three conditions must exist for CISCC to occur: tensile stress, a corrosive environment, and susceptible material (Figure 1). These conditions must be understood and accounted for when evaluating CISCC susceptibility. Furthermore, non-obvious factors, such as surface conditions and geometric confinement, can significantly affect the intensity of one or more of the three listed conditions for CISCC.

Cold spray provides a corrosion barrier coating that has the added benefit of generating compressive residual stresses in the coating and the material immediately beneath the coating. This effectively removes two of the three conditions required for CISCC. For the sensitized material around the welds beneath the coating, the two removed conditions are exposure to corrosive environment and tensile

stresses. For the cold spray coating, the two removed conditions are tensile stresses and susceptible material.

1.6 Properties

High CISCC resistance of nickel and nickel-based alloys has been reported by industry and academia (Alloys 2020; Haynes 2020). Various metal vendors report CISCC data correlating CISCC resistance to the fraction of nickel contained in each alloy. Discussion of cold spray properties in the paragraphs below is relative to common canister materials (SS 316 and SS 304) and nickel-based alloys.

In 2012, Westinghouse reported results from exploratory testing done to evaluate the use of HPCS for prevention of pressurized water reactor primary water SCC (Lareau et al. 2012). Cold spray coating of commercially pure (CP) nickel was applied to Inconel Alloy 600 substrates. Cyclic fatigue was evaluated with four-point bend testing; 50,000 cycles with 22.5 ± 21 ksi tensile stress loading was applied. Non-destructive evaluation (NDE) and scanning electron microscopy (SEM) work showed no cracking or debonding. Thermal cycling was done by heating coated samples to 400°C and plunging them into water. After 100 cycles no indications of cracking or debonding were found using NDE techniques and SEM. Impact testing was done with a round-nosed weight with 10J of energy. No cracking or spalling was observed. Vickers hardness testing performed on polished cross sections of coating showed remarkable consistency in hardness (~250 Vickers hardness number).

Adhesion testing was done using epoxy-based pull tests. The epoxy failed at ~10 ksi. This means the cold sprayed CP nickel has an adhesion strength of at least 10 ksi.

Doped steam SCC testing was done at 750°F, 5–13 psia H_2, 80 ppm of F-, Cl- and SO_4^{2-}. CP nickel coated and uncoated strain-hardened $^1/_8$-in. Inconel Alloy 600 and ¼-in. thick Inconel Alloy-182 clad bend bars were tested. Specimens were put into a four-point bend fixture and samples of each coating/thickness combination were tested at 70, 75, and 80 ksi tensile stress. All uncoated samples failed within 200 hours. Testing stopped after 800 hours for the ¼-in. samples and after 1,000 hours for the $^1/_8$-in. samples. No cracking was observed in the coated specimens. Although these tests are not representative of DCSS canisters, these tests provide evidence of the potential benefits of cold spray coatings.

For alloys that have high melting points, best properties are achieved by cold spraying under the following conditions:

1. An HPCS system is used.
2. Helium is used as the carrier gas.
3. Surface preparation is done correctly.
4. The correct material is selected for the application.
5. Powder is processed correctly.
    a. Sieving powder to remove fines.
    b. Drying powder.

For alloys with high melting points, much of the cold spray work that has been done is for coating of jet turbine blades and natural gas power generation turbine blades. These blades operate at temperatures of 1,000°C and higher while rotating at speeds greater than 10,000 rotations per minute in corrosive combustion environments. Competing General Electric and Siemens patents exist in the cold spray patent space related to the coating of gas turbine blades. Inconel 718 is an alloy of interest for gas turbine blades. Some reported values for the properties of cold sprayed Inconel 718 are shown in Table 1 below. These numbers come from several universities that used nitrogen (N) as the carrier gas for cold sprayed coupons. Using helium as the carrier gas produces superior properties in cold spray coatings. Information

about commercial cold spray coatings for natural gas industries are typically trade secrets and likely have properties superior to what is reported in Table 1 below.

Cold spray coatings that feature high hardness and strength are being developed to replace electroplated chrome and Ni for U.S. Department of Defense (DoD) combat systems. Properties for one such cold spray coating, Ni and CrC-NiCr blend, are listed in Table 1 below. These DoD cold spray coatings are designed to produce greater resistance to corrosion and greater wear resistance than electroplated chrome coatings.

Table 1. Cold spray property values from various sources.

Coating Material	Substrate Material	Carrier Gas	Bond Strength (KSI)	Hardness (HV)	Porosity (%)	Residual Stress (psi)	Ultimate Strength (KSI)	Reference
SS 304	SS 304	N_2/He (25/75)	>~12[(a)]	450	0.07	-50.8 to -65	-	(Yeom et al. 2020)
Inconel 718	SS 316	-	-	507	0.25	-	67	(Luo et al. 2018)
Inconel 718 PWHT	SS 316	N_2	-	~410	<0.5	-	158	(Luo et al. 2018)
Inconel 718	Inconel 718	N_2	>~12[(a)]	-	<2	-29,008 to -58,015	-	(Fiebig et al. 2020)
Ni, CrC-NiCr blend	-	He	38	400-500	<0.5	-	-	(Nardi et al. 2019)

(a) Denotes that epoxy-based adhesion tests were performed and the epoxy failed before coating.

It should be noted that cold spray is an approved repair process for dozens of DoD applications. Cold spray repaired components have been in service on various military aircraft and naval vessels for nearly a decade (Champagne 2018). Cold spray is also used for repair of commercial aircraft components. Companies such as Detroit Diesel use cold spray to repair/rebuild commercial freight engines. These successful applications demonstrate long-term performance when exposed to corrosive environments and other degradation mechanisms. While these conditions are not representative of DCSS conditions, they set a precedent for long-term performance in corrosive environments.

1.7 Application

Cold spray is appropriate for in situ repair/mitigation of existing canisters, new canister fabrication, and final disposal storage systems. Cold spray can be used to deposit metal that acts as a corrosion barrier over fabrication welds and their HAZs or to coat the entire outer surface of canisters. Cold spray will have a relatively easy path to commercialization because of the significantly reduced regulatory requirement of coatings compared to other processes, such as welding, for DCSS canisters(Ross et al. 2021).

1.7.1 Surface Preparation

Surface preparation is important to ensure high adhesion. Grit blast, wire brush/wheels, scotch bright, grinding, machining, and low-velocity spraying with cold spray powder are all methods that can be used for surface preparation. Cold spray can be done without any surface preparation, but adhesion values will be significantly reduced.

For factory cold spray, grit blasting is a common surface preparation method. Blast medium material and size need to be carefully selected to avoid embedding blast medium in the substrate. For field cold spraying, Scotch-Brite™ or a wire brush/wheel work well. For robotic crawler repair application in rad environments, cold spray powder at low velocity, such that it acts like grit blasting media, is the simplest solution relative to robotic crawler design. However, this method generates powder that does not stick to the substrate and may need to be cleaned up. Integrating machining or grinding wheel systems into the robotic crawler is feasible and reduces the waste generation. If robotic crawlers are designed to grind out machine damaged areas, they can be used for surface preparation with minimal or no modification.

1.7.2 Methods of Application

For factory HPCS of new canisters, large industrial systems with liquid-cooled nozzles can produce high-quality cold spray deposits economically. Helium recycling in factory cold spray enables improved quality at reduced cost (Howe 2017). Similar processes can be used in a dedicated processing facility for spent nuclear fuel canisters.

Field equipment for HPCS is a relatively new development by Army Research Lab and VRC Metal Systems. Recently, Army Research Lab has demonstrated HPCS with clearances as small as 1.5 in. using blended Ni and CrC-NiCr powder with helium carrier gas. Porosity less than 0.5% and bond strength of 29 ksi was achieved (Nardi et al. 2019). The nozzle shown in Figure 5 was used. Nozzles designed for very low clearances have a bend that results in reduced velocity of the gas stream. The exact same material sprayed with a straight nozzle has 38 ksi adhesion compared to 26 ksi achieved using the angled nozzle.

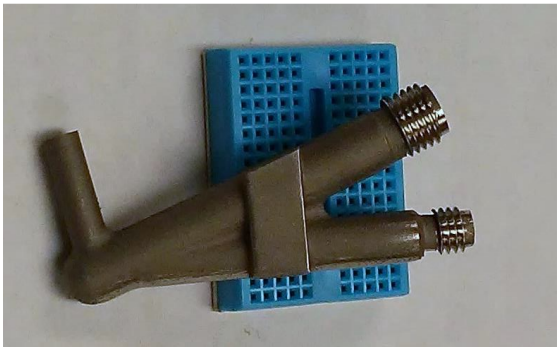

Figure 5. Miniature angled Cold spray nozzle capable of spraying a 1.5-in. inner diameter of a pipe (Nardi et al. 2019) designed by Army Research Lab. Image provided by Army Research Lab.

Miniature angled nozzles for spraying in confined spaces have significantly lower velocities due to the direction changes of the gas stream. Therefore, materials that can typically be sprayed with N_2 using a straight nozzle require He gas when using an angled nozzle (Nardi et al. 2019). Collection and removal of non-deposited powder is a consideration and may be required canister repair.

As part of a Small Business Innovation Research award from the DOE, VRC Metal Systems and their team demonstrated the ability to deposit SS and Inconel powders on SS 304L such that galvanic potential is matched and resistance to pitting is improved. A robotic crawler in a confined environment, representative of the space between a DCSS canister and overpack, executed HPCS using crude manual controls as a proof-of-concept demonstration. This work established the technical viability for cold spray mitigation and repair within the overpack using remote robotic equipment. Results are shown in Figure 6 below.

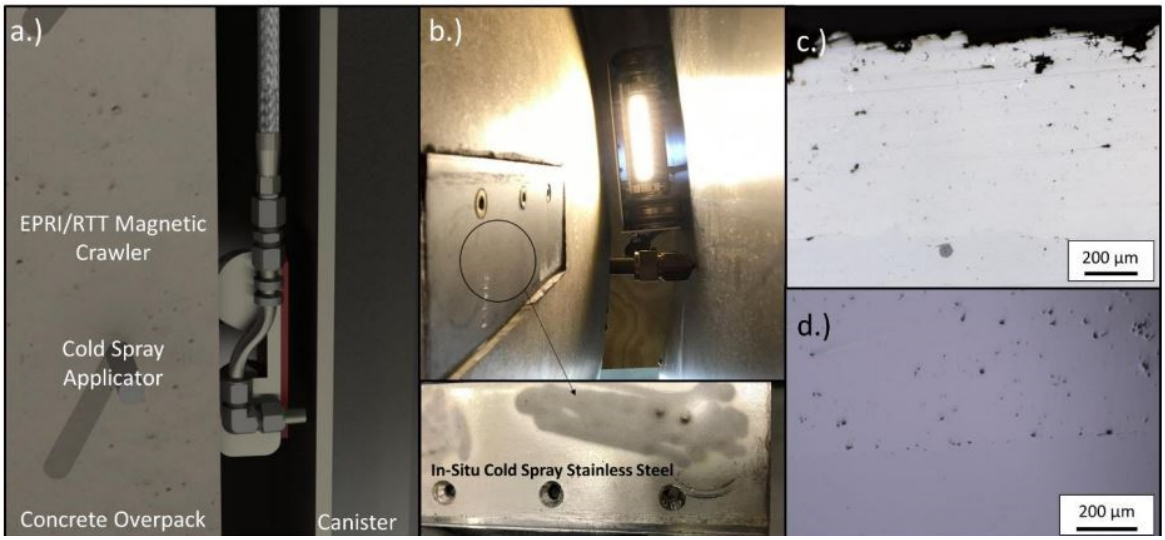

Figure 6. (a) Graphic of in situ cold spray repair; (b) photo of cold spray mockup trail with Electric Power Research Institute – Robotic Technologies of Tennessee robotic crawler showing the viability of in situ stainless steel cold spray; (c) cross section of cold sprayed SS 316L; and (d) cross section of Inconel 625. Provided by VRC Metal Systems.

For situations where tight clearances do not exist, portable cold spraying can be done by manual handheld operation. Alternatively, the processes can be controlled using computer numerical control (CNC) by mounting portable equipment on a portable industrial robot arm.

1.8 Degradation Mechanisms

When best practices are followed, HPCS coatings can far outlast the austenitic SS base metal. This is because more resilient materials, such as Ni, can be used and compressive residual stresses are induced. The interface between the cold spray coating and base material that is exposed to the environment is an area of concern. Coating material needs to be properly selected and tested to ensure significant galvanic potentials do not exist between the coating and substrate materials.

Geometric effects need to be considered to ensure crevices or detrimental surface textures are not produced. The presence of crevices or rough surface textures could accelerate the onset of CISCC. All instances of CISCC in the fielded nuclear applications reported by the Pressurized Water Reactor Owners Group (Hosler and Hall 2010; Lareau 2014) were associated with crevice corrosion. This can be avoided by cold spraying to seal crevices.

Surface texture in cold sprayed coatings is affected by process parameters and powder preparation.

1.9 Cold Spray for Life Extension Recap

HPCS is appropriate for in situ repair/mitigation of existing canister and new canister fabrication. HPCS can be used to deposit metal that induces compressive residual stresses and acts as a corrosion barrier over fabrication welds and their HAZs. Nozzles that are capable of spraying in areas with clearances as small as 1.5 in. are developed (Nardi et al. 2019) (Figure 5). Forces and temperatures required during the cold spray application are very low. Regulatory requirements for coatings are light compared to other technical areas, such as design or welding, for DCSS canisters. This will enable faster commercialization of the cold spray technology.

Benefits of cold spray include the following:

- Excellent mechanical properties can be achieved (>100 ksi [689 MPa] tensile strength, >30 ksi [207 MPa] adhesion strength).
- There is no deposition thickness limit.
- Below 1% porosity can be achieved. No interconnected porosity is produced.
- HPCS produces a high-density, high-hardness, deposit with compressive residual stresses as opposed to the tensile residual stresses associated with melt/fusion-based processes. This retards crack propagation and improves the CISCC resistance like shot peening.
- The process is inspectable using standard NDE techniques (Glass et al. 2018).
- Factory-based, field portable and robotic crawler cold spray systems are demonstrated or fully commercialized configurations.

Successful cold spray applications in other industries have resulted from significant research efforts and understanding to optimize the cold spray process for specific applications. Nevertheless, a significant amount of work needs to be done to develop HPCS for DCSS canister repair and mitigation, including the following research activities:

- Develop an understanding of and the interface between the coatings and substrates when exposed to the service environment
- Optimize coating chemistry for CISCC resistance and avoidance of galvanic effects
- Verify coating integrity in canister sliding and scraping conditions
- Develop an understanding of how surface roughness/texture developed by cold spray, and post processes such grinding or buffing, affects CISCC initiation
- Reduce nozzle clogging and improve deposition efficiency for in situ repair
- Optimize process for stationary equipment
- Optimize process for field repair conditions
- Quantify mechanical and thermal properties
- Perform additional mechanical testing to support structural modeling and analysis of cold spray coated components.

The work above will result in cold spray process parameters and chemistries designed and optimized for CISCC repair and mitigation of DCSS canisters. Additionally, execution of the work above will enable a broad understanding of the cold spray processes relative to CISCC resistance, identification of optimal material systems, and documentation of best practices and technical datasets needed by stakeholders to implement, evaluate, and regulate cold spray repair and mitigation of CISCC. A more thorough discussion of needed development work is included in sections 2.3-4.

This page is intentionally left blank

2 Fiscal Year 2021 Progress

This year test coupons were cold sprayed using various powder alloys and carrier gasses. Mechanical testing, characterization and corrosion testing was completed for a subset of cold spray process conditions. Results and analysis for the completed subset of samples are presented below. Testing continues for additional process conditions.

Learnings from this exploratory work highlight knowledge gaps relative to corrosion behavior at the coating/substrate interface exposed to the environment. Exploratory work demonstrates significant differences in properties and performance based on carrier gas, chemistry, and whether or not the surface of the coating was polished. Pitting tests highlight the potential for galvanic effects at the exposed coating/substrate interface.

2.1 Cold Spray Coating of Test Samples

Cold sprayed test coupons were made by depositing powders using materials listed in Table 2 on SS plate substrate using various processing conditions. Iterative coupon generation and testing will continue until the project team identifies optimal process parameters for high-fidelity DCPD CISCC testing and analysis.

Table 2. Elemental composition for powders used. Only elements that make up at least 0.1% or greater of at least one of the powders are shown

	Inconel 625	316 SS	Super C	CP Ni	CRC-410	CRC-300
C	0.01%	<0.001%	0.02%	-	4%	10%
Cr	21.19%	16.81%	23%	-	Balance	Balance
Ni	Balance	11.92%	Balance	>99.9%	8%	21%
Mo	9.1%	2.43%	17.7%	-	-	-
Mn	0.04%	0.99%	0.7%	-	-	-
Si	0.07%	0.36%	0.5%	-	0.3%	-
Fe	3.94%	Balance	0.6%	-	0.1%	-
Al	0.10%	-	-	-	-	-
Nb	3.68%	-	-	-	-	-
O	1.94%	0.05%	-	-	-	-
V	-	-	0.30%	-	-	-
W	-	-	0.26%	-	-	-
V	-	-	0.30%	-	-	-

2.1.1 Alloy Powder

CP Ni, Inconel 625, and Super C powders were deposited onto SS304/304L to create test samples. Cold spray powders were deposited in lengths along the plate as shown in Figure 7a. Deposits were made using nitrogen carrier gas and helium carrier gas. For each material-carrier gas combination, deposits were made with masked edges, which produces cliff-like interface between the cold spray and base metal, and a blended edge, which produces a tapered interface between the cold sprayed layer and the base metal. Examples for coupons cut from masked and unmasked deposits are shown in Figure 7b. Samples were sprayed with (CP) Ni, Inconel 625, and Super C cold sprayed using N2 carrier gas. Additionally, Inconel 625 coating was also deposited using He carrier gas for comparison. All these coatings are compared to

the SS substrate. Fabrication of CP Ni and Super C coupons sprayed with helium carrier gas are in process.

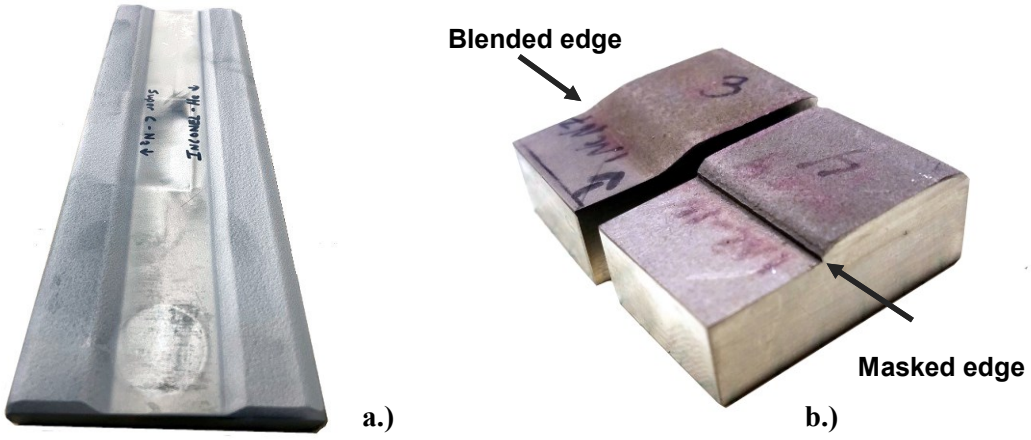

Figure 7. Single alloy cold sprayed plates and samples. a) A plate with Super C sprayed with nitrogen carrier gas and a blended edge is on the left side of the plate. Inconel sprayed with helium carrier gas and a blended edge is on the right side of the plate. b) Test coupons cut from plates with blended and masked edges.

2.1.2 Blended Powder

Hard particles can be added to a cold spray powder to enhance bond strength, reduce porosity, prevent nozzle clogging, and increase mechanical wear resistance of deposited material. For the purpose of this report, the matrix material refers to the metal or metal alloy that makes up the majority of the deposited material. Hard particles can be hard metal alloys but are more commonly ceramics. When cold spraying a blended powder, the deposition efficiency of the hard particles is typically much less than the alloy matrix material Chrome carbide (CrC) is a popular hard particle material for blended cold sprayed powder. Blended powders are important for in situ DCSS canister work because they enable cold spray in tight spaces. Cold spraying in tight spaces often requires angled nozzles. The velocity drop associated with the direction change significantly reduces particle velocity. This means there is much less energy available at impact. Hard particles act as battering rams and provide additional plastic deformation of matrix material needed to get desired properties when spraying with angled nozzles. Angled cold spray nozzles are discussed in more detail in section 1.7.2. For the purpose of this report, hard particles refer to particles with significantly higher hardness compared to the matrix material to witch they are added for the purpose of increasing plastic deformation upon impact, preventing clogging, or enhancing mechanical wear resistance of the resultant deposit.

Cold spray samples sprayed using Inconel 625, Super C, and CP Ni were sprayed with various ratios of CrC-300 and CrC-410. Figure 4 shows blended powder coupons sprayed in FY21. Testing and analysis of these blended powder samples will occur early in FY22.

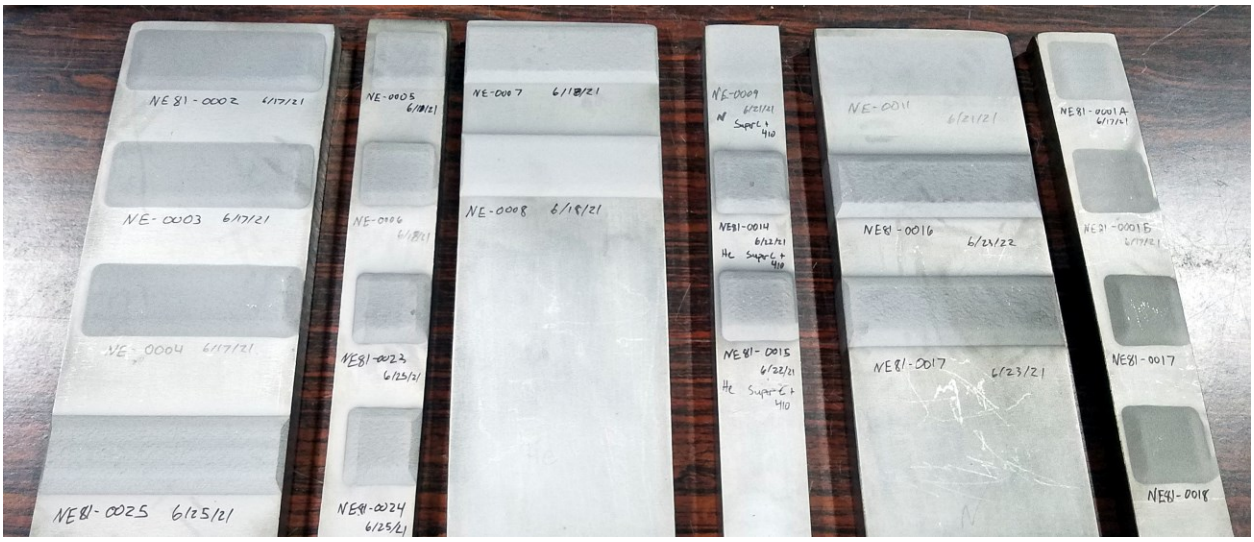

Figure 8. Cold sprayed coupons sprayed with metal alloy powder mixed with chrome carbides resulting in a cermet cold spray deposit. These samples were created late in FY21. Testing of these cold sprayed deposits will occur early in FY22. Data, analysis, and processing details will be presented in FY22 reporting.

2.2 Mechanical Properties

Completed mechanical testing for cold sprayed Inconel Alloy 625, CP Ni, and Super C (like Inconel but with higher molybdenum content) is reported in the sections below. Generated cold spray samples exceeds strength limitations of current ASTM adhesion tests because the epoxy used fails before the cold sprayed coating fails. Because all cold sprayed coatings tested thus far exceeded the limits of standard adhesion testing, micro tensile test specimens will be generated to determine ultimate adhesion strength using the ASTM E-8 tensile testing standard. Initial adhesion-based testing is for a quality control tool. For cold spray processes of interest, failure of the glue indicates proper surface preparation and process controls. Failure or debonding of the coating prior to glue failure would indicate the process is out of control.

2.2.1 Materials and Methods:

The cold spray coatings were tested for Vickers hardness, porosity, wear, and roughness. The coatings consisted of CP Ni, Inc 625, and Super C, which were deposited using N_2 carrier gas. Additionally, Inc 625 coating was also deposited using He carrier gas for comparison. All these coatings were compared to the SS substrate. Fabrication of CP Ni and Super C coupons sprayed with helium carrier gas are in process.

The Vickers hardness of the coatings at room temperature was measured ex-situ with a Model FM-ARS9000 fully-automatic Vickers microhardness testing system. The hardness parameters were 500gf at 12 second dwell time with a 0.250 mm spacing in both the x and y axes. Areas of indentions were selected in a 6 × 5 matrix across the cross section, with at least 30 indents per sample, to determine average hardness values.

The porosity of the cold sprayed coatings was evaluated using ASTM standard E2109 (E2109-01(2014) 2014). At least three optical micrographs were collected using similar magnification to obtain representative porosity measurements throughout the length and thickness of the coating. Porosity measurements were obtained using ImageJ software (Schneider et al. 2012) and are reported as the percent porosity by area.

Dry linear sliding reciprocating wear tests were conducted using an Anton Paar pin-on-disk tribometer. Hard Si_3N_4 balls with a diameter of 6.35 mm were selected as the counterface material to minimize ball wear. All tests were performed using a sliding velocity of 100 mm/s, up to 4,000 cycles, which corresponds to a sliding distance of 165 m, and a normal load of 1 N, which correlates to a 0.7 GPa maximum Hertzian contact stress for Ni-based alloys in open air with a relative humidity of ~40%. Keyence VR 5100 white light interferometry measurements were used to determine the surface roughness and volumetric loss of material by wear. The wear volume was then divided over the normal load and sliding distance to obtain specific wear rates in $mm^3/N \cdot m$.

2.2.2 Vickers Hardness of Cold Spray Coatings:

The most common parameter used to describe a material's resistance against wear is the hardness of the material. Hardness is defined as a material's resistance against plastic deformation. Figure 9 (a) shows the Vickers microhardness values measured as a function of depth at room temperature (RT) from near-top surface of the Ni-based cold spray coatings to their corresponding SS substrate. It was observed that there is no significant change in the hardness as a function of depth, which can attribute to homogenous distribution of particles upon deposition. Figure 9 (b) summarizes the average microhardness of all the cold spray coated samples, which were also compared to the stainless substrate. All the coatings show about a ~2–3X increase in hardness when compared to that of the substrate. The Ni coating exhibited an average hardness of 263 HV at RT, which is within the range of the hardness values reported in literature for Ni (Alidokht et al. 2016; Torgerson et al. 2018). The Inconel 625 coatings exhibited a higher hardness than Ni coatings and other hardness values reported for bulk Inconel 625 alloy in literature (Günen et al. 2017).

Inconel 625 sprayed with helium is has the highest hardness. This is likely due to the fact that the small helium atom has a much higher critical velocity compared to nitrogen and therefore there is significantly more energy available upon particle impact due to the squared velocity term in the kinetic energy equation This increase in kinetic energy produces additional extreme plastic deformation at particle boundaries and greater cold working of previous layers. The end result is increased interparticle bonding and higher hardness compare to similar alloys sprayed with nitrogen. Super C sprayed using nitrogen carrier gas, Super C (N_2), coating showed a better hardness than that of Inconel 625 sprayed with N_2 carrier gas, Inconel 625 (N_2). This is hypothesized to be due to the increased molybdenum and carbon content compared to Inconel 625(N_2). The hardness of Super C (N_2) was lower than Inconel 625 (He). However, we anticipate the Super C sprayed with helium will have higher hardness than Inconel sprayed with helium carrier gas due to increased work hardenability associated with higher molybdenum content.

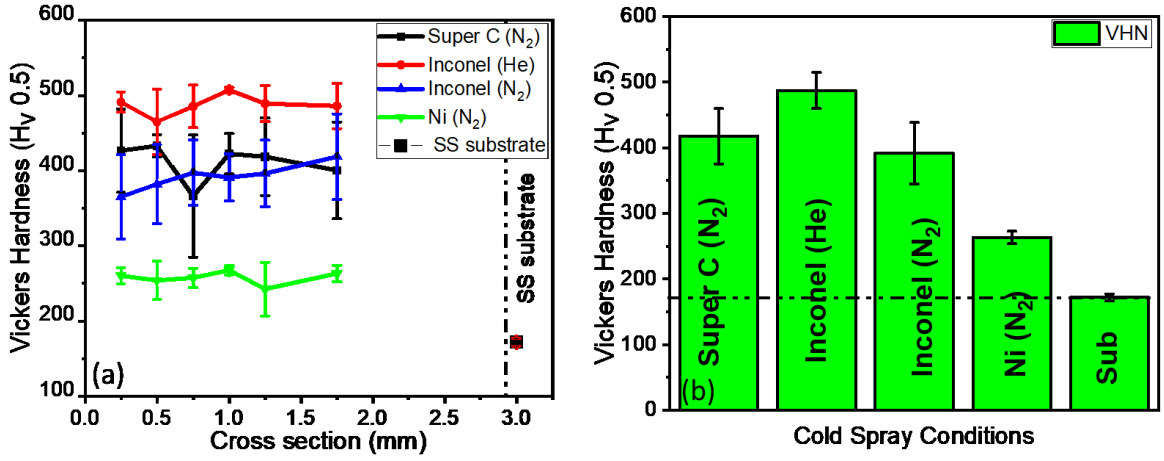

Figure 9. (a) Cross-sectional Vickers hardness of various colds spray coatings under different gas environments and (b) average Vickers hardness values of various cold spray coupons and SS substrate.

2.2.3 Surface Roughness and Porosity of the Cold Spray Coatings:

In applications that include direct use of cold sprayed coatings without any machining, the surface roughness of the coating could play an important role in the reliability of the coating life. The resultant surface roughness (S_{a1}) is a combination of many factors, such as powder particle size distribution, morphology, as well as the process parameters and is considered an indirect indicator of the coating density and coating process integrity. Surface roughness is used as a characterization tool during process optimization. Table 3 shows S_{a1} of the various cold spray coatings produced under different gas environments such as N_2 and He. It was observed that the coating under the He environment results in lower S_{a1} when compared to that of the coatings under the N_2 environment. S_{a2} represents the average surface roughness values after specific machining and polishing was done for further tribological characterizations. Tribological tests were conducted in samples both with and without polishing to evaluate the effect of surface roughness on the wear properties of these coatings. The results are presented in Table 3.

Figure 10 (a, c) displays the bright field, low magnification cross-sectional optical micrographs of Super C (N_2) and Inc-625 (He) cold spray coatings. It was observed that each powder type resulted in the formation of dense coatings, although multiple triple junctions and other pores/inclusions were present. This can be attributed to various reasons, such as relatively low hardness, various deposition parameters, including the particle velocity, and lower oxygen content. The corresponding bright field optical micrographs were processed to calculate the density of these inclusions/pores that were shown in Figure 10 (b, d) with the red patches. Average porosity is summarized in Table 1. Inc-625 (He) has the lowest porosity among all the cold spray coatings (~1%). Improved properties of powders sprayed with He is due increased kinetic energy of particles due to higher velocities produced by helium carrier gas compared to nitrogen carried gas. Increased kinetic energy upon impact produced improved particle to particle bonding.

Table 3. Surface roughness of the cold spray coatings before (S_{a1}) and after (S_{a2}) polishing and roughness of the wear tracks before (S_{w1}) and after (S_{w1}) polished coatings

Sample	Porosity (%)	S_{a1} (µm)	S_{a2} (µm)	S_{w1} (µm)	S_{w2} (µm)
Super C (N_2)	5.51 ± 0.44	16.7 ± 0.5	1.6 ± 0.09	12.0 ± 0.6	0.2 ± 0.06
Inc-625 (He)	1.21 ± 0.20	15.7 ± 0.5	3.12 ± 0.19	13.9 ± 0.7	0.31 ± 0.04
Inc-625 (N_2)	5.79 ± 0.18	17.2 ± 0.6	4.6 ± 0.2	12.4 ± 0.6	0.25 ± 0.05
Ni (N_2)	3.78 ± 0.59	18.5 ± 0.6	1.3 ± 0.08	9.8 ± 0.5	0.73 ± 0.06

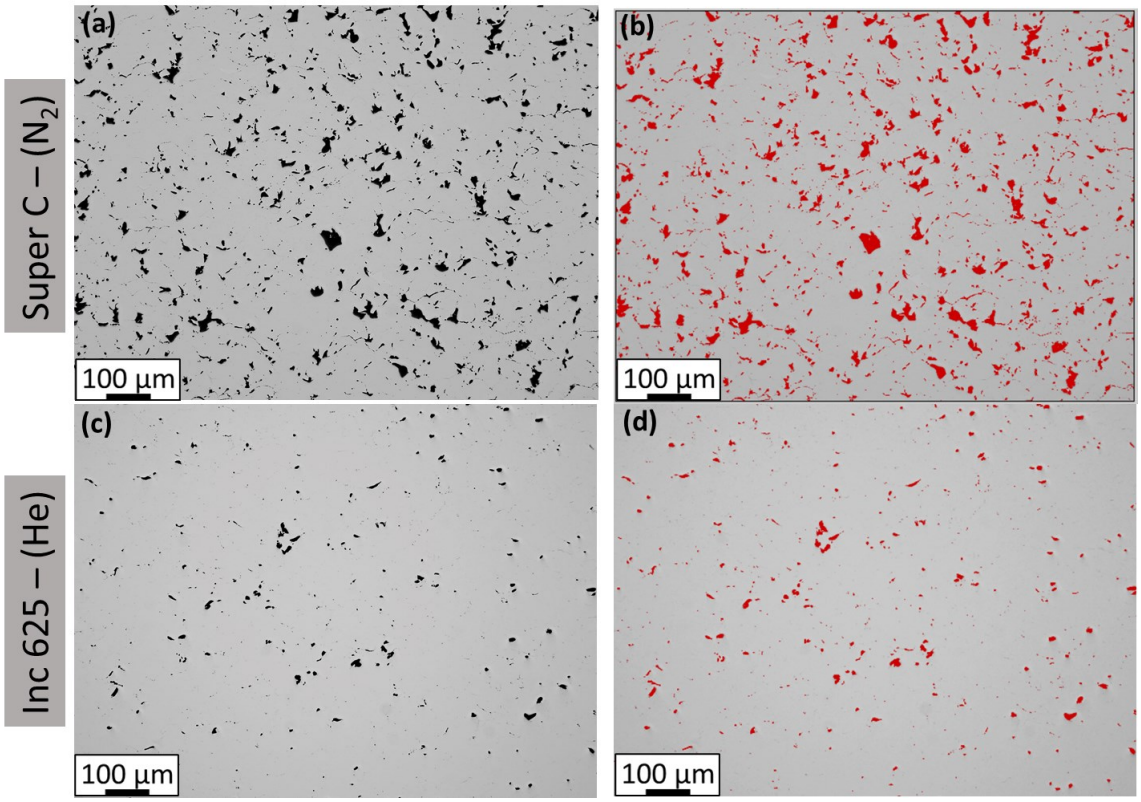

Figure 10. (a, c) Bright field, low magnification optical micrographs of the cold spray coatings showing pores/inclusion dark regions; (b, d) pores being covered with the red regions for calculating the average density of pores/inclusions for the corresponding bright field optical micrographs.

2.2.4 Friction and Wear Rate of the Cold Spray Coatings:

Typical sliding reciprocating coefficient of friction (CoF) curves of cold spray coatings tested at RT for both bare and polished surfaces are shown in Figure 11. Test were performed in compliance with ASTM G-113 (ASTM-G113 2016). All the bare coatings exhibited a long initial run-in period for the first 400 to 800 seconds, as shown in Figure 11(a), before reaching steady-state values, showing extreme values of ~0.2 and 0.4 for Inc-625 (He) and Super C (N_2) coatings, respectively. The variation and instability in the CoF curves during the run-in period can be attributed to large variation and unevenness in the surface roughness (S_{a1}, S_{w1}) upon and after sliding. On the other hand, for the polished/machined samples, the initial run-in period is relatively short, for the first 150–200 seconds of sliding time, before attaining the

steady state CoF values as shown in Figure 11(b). The early steady state CoF is also attributed to lower surface roughness and relatively smooth frictional forces acting on the body upon sliding. In comparison, the CoF of SS substrate is also shown in Figure 3(b).

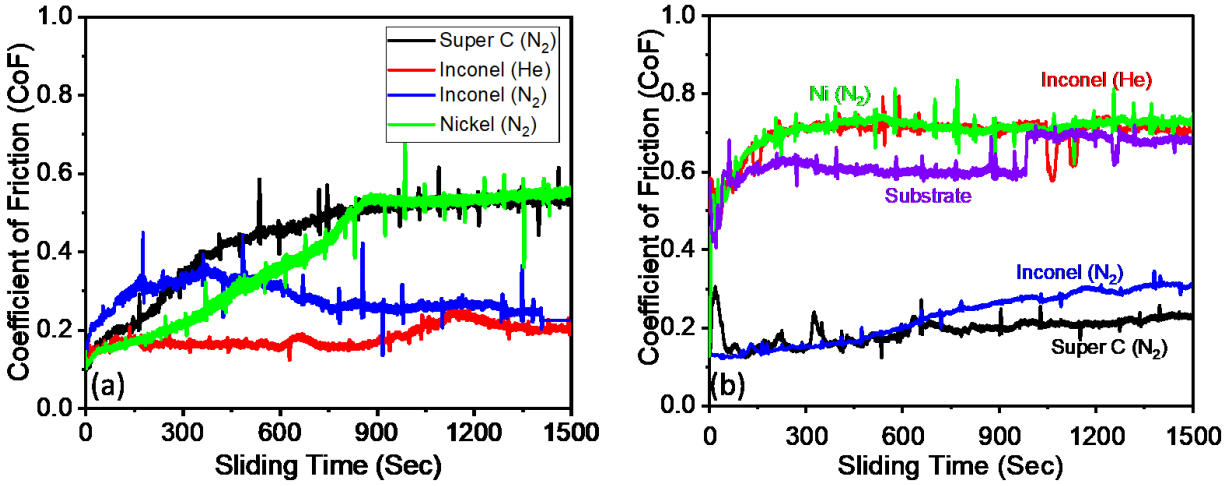

Figure 11. (a) Representative CoF versus sliding time at RT of bare cold sprayed coatings; (b) CoF versus sliding time at RT of polished cold sprayed coatings.

Figure 12 summarizes the CoF and wear rates of the bare and polished cold spray coating tested at RT. It was observed that the CoF of Super C (N_2) and Inc-625 (N_2) are lower (~ 0.2) in polished conditions than that of the bare coatings. On the other hand, Inc-625 (He) and Ni (N_2) showed higher CoF values (~ 0.7) in the polished conditions than that of the bare coatings, which is in agreement with the literature values [4]. In addition, the CoF values of Super C (N_2) and Inc-625 (N_2) are three times lower to that of the substrate's CoF. The bare coatings showed lower CoF because the larger surface roughness, where the particles adhered with high protrusions were subjected to true contact leading to reduction in contact area upon sliding which are discontinuous, because of which the steady state was difficult to achieve. Super C (N_2) showed the lowest CoF in polished condition because of the high hardness of the coatings resulting in lower frictional contact caused by a reduction in the sliding contact area. The specific wear rates of the cold spray coatings were determined after 165 m of sliding distance to assess the tribological performances. The wear rates of the cold spray coatings along with the substrate properties in the polished condition are shown in Figure 12 (b). It was interesting to observe that the wear rates of the polished/machined coatings are almost an order magnitude lower than that of the bare coatings, which is mainly attributed due to large variation in surface roughness and coherent contact area upon sliding. In addition, within the polished sections, the wear rate of these polished cold spray coatings showed almost an order of magnitude lower wear rates than that of the substrate material, which is due to relatively high hardness of the coatings. Not all coatings follow the Archard's law (Archard 1953), where the wear rate is inversely proportional to the material's hardness but also depends on the morphology, structure, and deposition parameters.

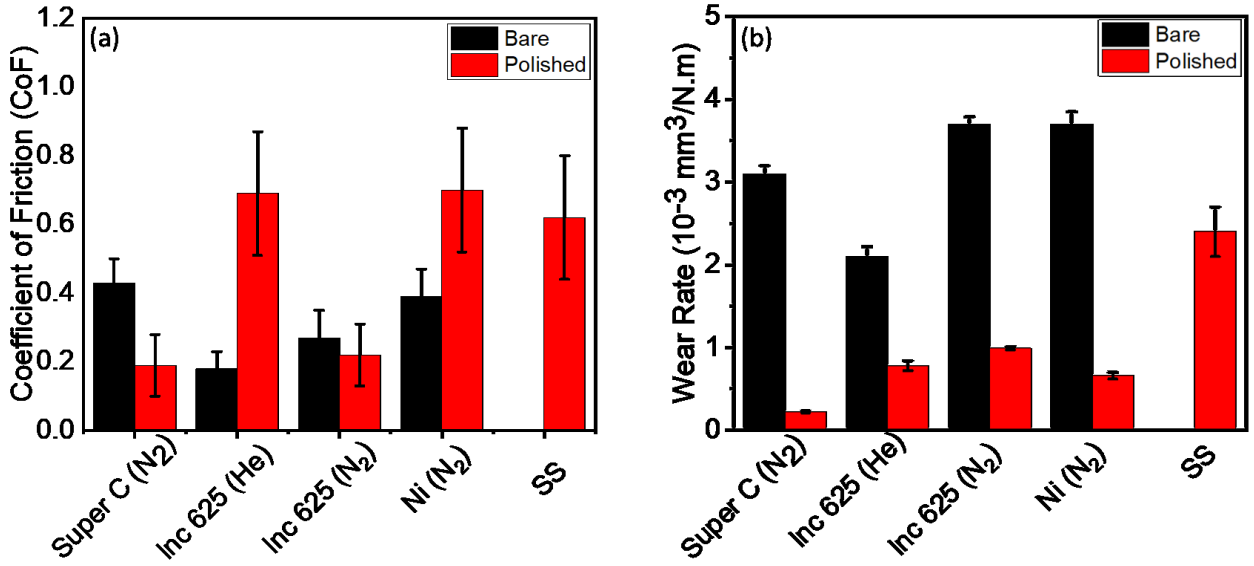

Figure 12. (a) Steady state CoF of cold spray bare and polished coatings in comparison with the substrate (SS); (b) Wear rates of cold spray bare and polished coatings in comparison with the substrate (SS)

2.3 Corrosion Testing

2.3.1 Materials and Methods

Cold sprayed samples (example images in Figure 13) were analyzed through electrochemical and full immersion exposures to determine initial corrosion properties. The matrix of test coupons were painted with PEELSEAL green maskant. Coated and uncoated test coupons are shown in Figure 13. Samples were sent to SNL and analyzed for corrosion susceptibility through accelerated testing methods as noted in Table 4.

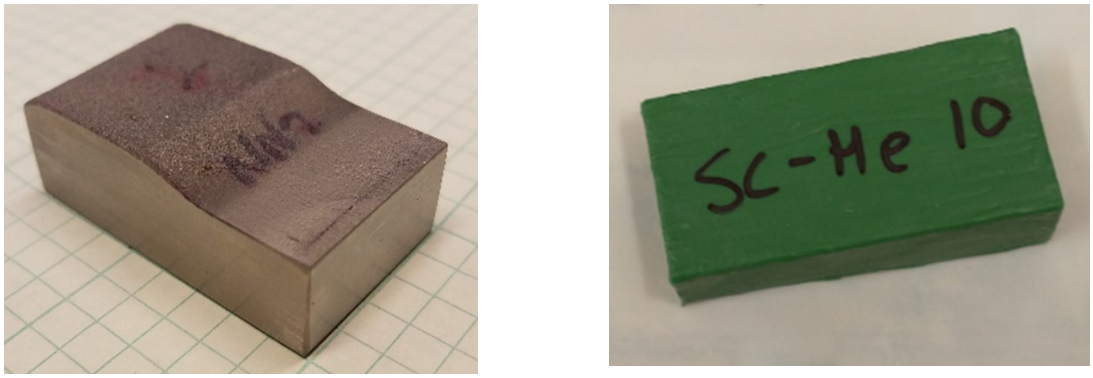

a) b)

Figure 13. a) Top view of unpainted test coupon. b) Bottom view of painted, PEELSEAL green maskant, test coupon. Bottom and sides of coupons were painted such that only the top surface will be exposed during pitting tests.

Table 4. Cold spray sample corrosion testing matrix.

CS Material	CS/Base metal Interface	Process Gas	Electrochemical Testing			Pitting Corrosion Test
			As-Sprayed	*600 grit*	*1200 grit*	
Inconel 625	Blended	He	X	X	X	X
Inconel 625	Blended	N	-	-	-	X
Inconel 625	Masked	N	X	X	X	X
Nickel	Blended	N	-	-	-	X
Nickel	Masked	N	X	X	X	X
Super C	Blended	N	X	X	X	X

2.3.2 Full Immersion Electrochemical Measurements

Corrosion behavior of the cold sprayed materials was evaluated by potentiodynamic polarization scans according to ASTM G5-14e1. Scans were performed on a Biologic SP-300 Potentiostat. Three sample surface finishes were evaluated for each cold sprayed material, including the as-sprayed, 600 grit, and 1200 grit finish. To achieve the 600 and 1200 grit finishes, a Pace Technologies Nano 2000 with silicon carbide grinding pads was used. After the grinding, samples were rinsed with deionized water and dried with nitrogen. Samples were tested in 0.6 M NaCl solution at RT (25 ºC) in a standard three-electrode flat cell configuration with an Ag/AgCl reference electrode and a platinum mesh/wire counter electrode. An o-ring was epoxied onto the sample using DevCon 5-minute epoxy. This o-ring was then epoxied onto the flat cell and secured with an Irwin Tools quick-grip clamp. All samples were measured at a minimum of three different locations in the cold sprayed area (Figure 14) for each surface finish. Electrochemical testing consisted of a one-hour observation of the open circuit potential (OCP) followed by a potentiodynamic polarization (PP) scan with a scanning rate of 0.167 mV/s, a voltage range of -0.2 to 0.8 V vs. Ag/AgCl, and a cutoff current at 100 μA. The area tested was optically measured after testing using a Keyence VHX-7000. The PP data was normalized by the surface area under testing and the OCP. The normalized PP curves for each sample were plotted and analyzed in Origin.

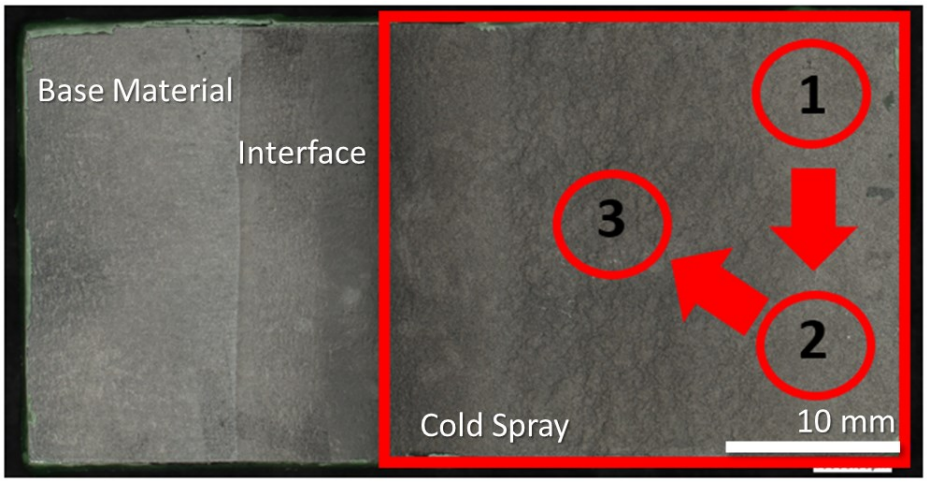

Figure 14. Representative CS sample with the red box indicating the CS area. The red numbered circles display the areas for corrosion testing of the top surface.

2.3.3 Ferric Chloride Pitting Corrosion Testing

To further understand the pitting corrosion behavior of the cold spray samples, accelerated full immersion pitting tests were performed in accordance with ASTM G48 Method A. This allowed for simultaneous evaluation of unpolished base material, interface, and cold sprayed regions (depicted in Figure 14) of each sample. Cold spray samples were placed in 6% by mass ferric chloride solution in full immersion for a total of 72 hours at a constant temperature of 22 ºC. Following the immersion, all samples were rinsed with deionized (DI) water to remove corrosion products and dried with nitrogen.

2.3.4 Microscopy Analysis

Samples were imaged using both optical and SEM techniques to assess pre-exposure sample surface condition and post-exposure corrosion damage. For optical imaging, a Keyence VHX-7000 Digital Microscope was used. Post-exposure optical images were acquired for samples that underwent electrochemical corrosion testing. Samples that underwent pitting corrosion testing were optically imaged pre- and post-exposure for comparison. Additionally, samples that underwent pitting corrosion testing were examined using a Zeiss Gemini 500 Field Emission SEM. Prior to SEM, all samples were rinsed with DI water and dried with nitrogen. Images were collected at an accelerating voltage of 20 kV with secondary and backscattered scans followed by using a Brucker X-Flash 6-60 Energy Dispersive X-Ray Spectroscopy (EDS). Three areas of each sample were analyzed: the base material, the cold spray interface, and the cold spray surface (Figure 14).

2.4 Corrosion Testing Results

2.4.1 Electrochemical Testing Results

A summary of the hour long OCP evaluations for each cold spray material condition collected with the corresponding PP curves are presented in Figure 15, Figure 16, and Figure 17. In all cases, the as-sprayed conditions (solid lines) exhibit more unstable behavior in the OCP and there is evidence of metastable pitting incidents in the PP curves. The samples ground to either 600 or 1200 grit (dashed and dotted lines) exhibited a smoother evolution in OCP. The OCPs also dropped as the surface oxides were removed during grinding; thus, as compared to the as-sprayed state, the surface is slightly more active. However, during the PP scans, the curves display smoother currents, indicative of a reduction in

metastable pitting. All scans are presented as compared to measurements of the base material (black line) in 25 °C 0.6 M NaCl solution. Optical images of the exposed surface of the coupons before and after coupons are shown in Figure 18 and Figure 19.

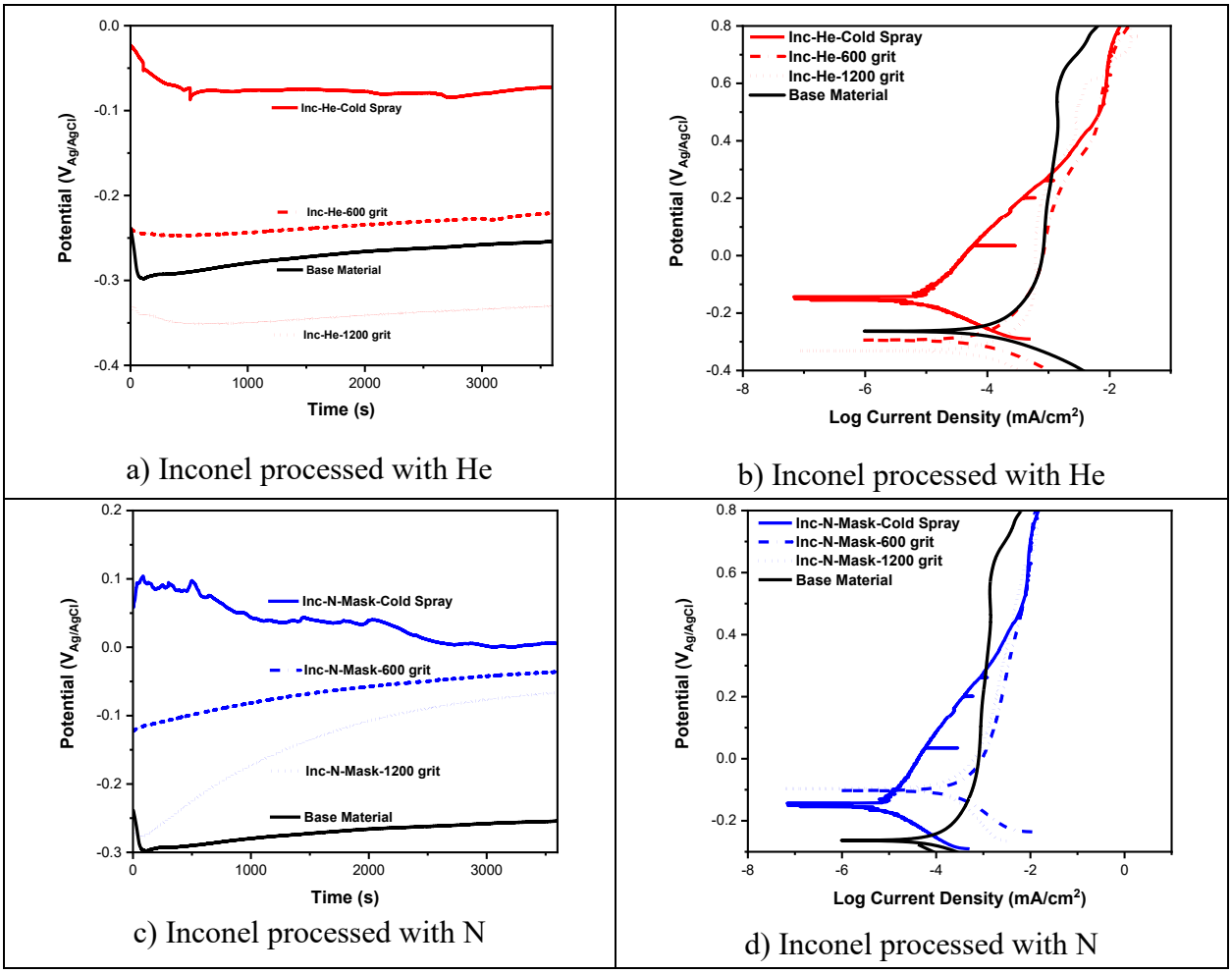

Figure 15. First set of images for summarizing electrochemical testing of the as-sprayed surfaces versus the 600 and 1200 grit ground samples as compared to the base material in 25 °C 0.6 M NaCl solution. One-hour OCP followed by PP for a) & b) Inconel processed with He, c) & d) Inconel processed with N. Image lettering continues in the next figure.

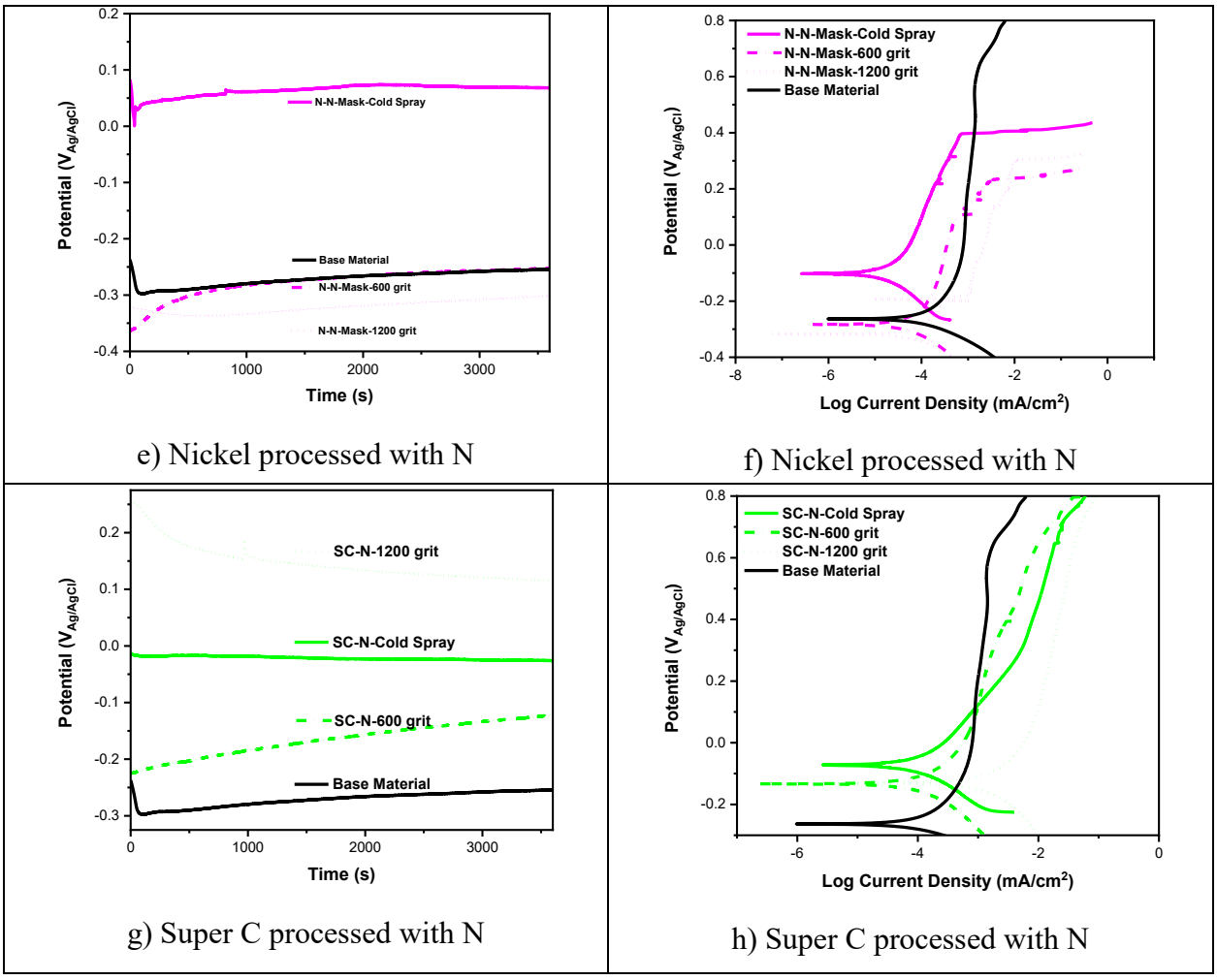

e) Nickel processed with N

f) Nickel processed with N

g) Super C processed with N

h) Super C processed with N

Figure 16. Second set of images for summarizing electrochemical testing of the as-sprayed surfaces versus the 600 and 1200 grit ground samples as compared to the base material in 25 °C 0.6 M NaCl solution. One-hour OCP followed by PP for e) & f) Nickel processed with N, and g) & h) Super C processed with N. Image lettering continued from previous figure.

A comparison summary of all cold spray samples examined is presented in Figure 17. All samples in the as-sprayed condition exhibit a roughly 200–350 mV higher OCP than the base material. The passive current densities displayed in the PPs range from roughly 5×10^{-4} to 5×10^{-2} mA/cm^2 as compared to the base material, which displays a passive current density of 1×10^{-3} mA/cm^2. However, more notable is the metastable pitting and bend-over potentials observed. All samples except for the Ni nitrogen samples did not exhibit a bend-over potential (Figure 17-b). The Ni nitrogen sample shows a bend-over at a potential of 0.4 V, indicative of the occurrence of sustained pitting or localized corrosion.

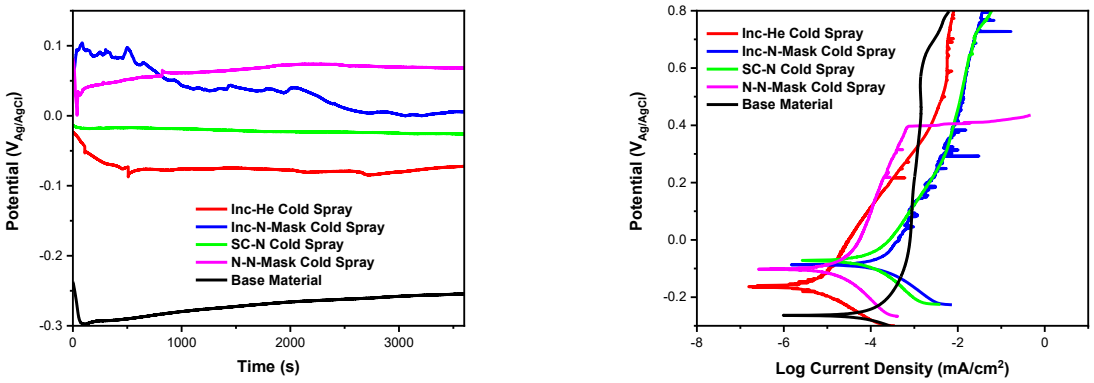

a) b)

Figure 17. Summary comparison of all as-sprayed CS samples; a) one-hour OCP and b) PP.

a) Inconel sprayed with He pre-exposure

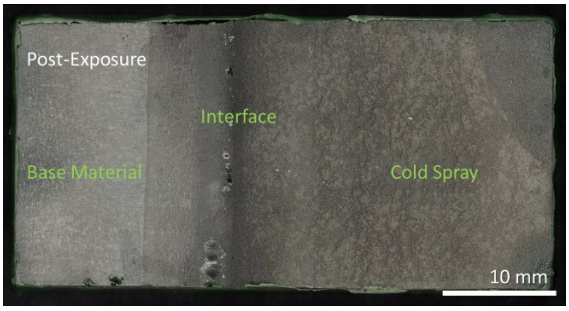

b) Inconel sprayed with He post-exposure

c) Inconel sprayed with N pre-exposure

d) Inconel sprayed with N post-exposure

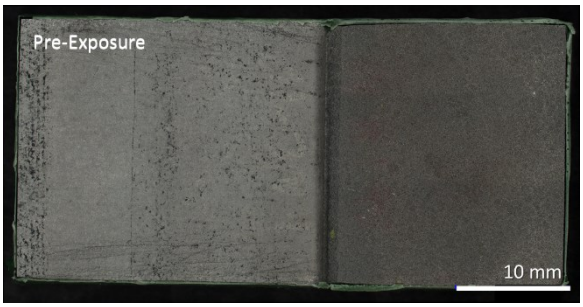

e) Inconel sprayed with N, masked interface, pre-exposure

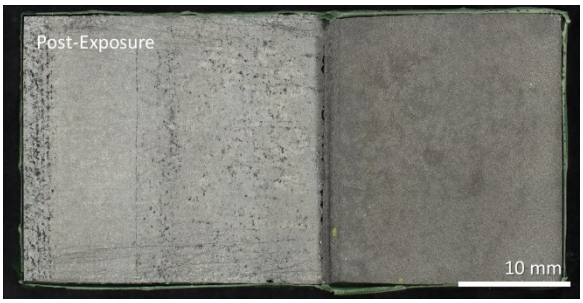

f) Inconel sprayed with N, masked interface, post-exposure

Figure 18. First set of optical images pre and post $FeCl_3$ 72 h exposure at 22 °C for a) & b) Inconel processed with He, c) & d) Inconel processed with N, e) & f) Inconel processed with N and masked. Samples are all oriented in the same direction as shown in b, with base material on the left and cold spray on the right of the image. Image lettering continues in the next figure.

g) Nickel sprayed with N pre-exposure

h) Nickel sprayed with N post-exposure

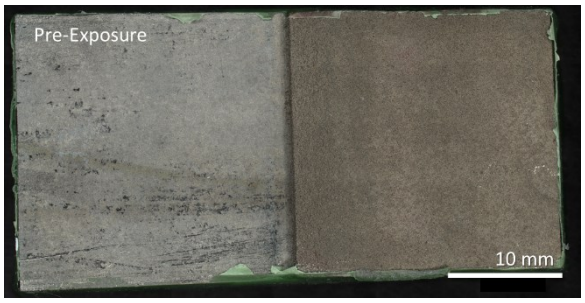

i) Nickel sprayed with N, masked interface, pre-exposure

j) Nickel sprayed with N, masked interface, post-exposure

k) Super C sprayed with N pre-exposure

l) Super C sprayed with N post-exposure

Figure 19. Second set of optical images pre and post $FeCl_3$ 72 h exposure at 22 °C for g) & h) Nickel processed with N, i) & j) Nickel processed with N and masked, and k) & l) Super C processed with N. Samples are all oriented in the same direction as shown in b, with base material on the left and cold spray on the right of the image. Image lettering continues from previous figure.

2.4.2 Pitting Corrosion Test Results

Pre- and post-exposure optical images of the FeCl3 full immersion exposures are presented in Figure 18 and Figure 19. As can be seen across all cold spray sample types and processing gasses, the interface region displayed the highest areas of attack (for both masked and blended samples). Additionally, notable differences are apparent between blended (Figure 19d & h) and masked (Figure 19f & j) interfaces regarding corrosion damage. In general, the cold sprayed regions presented relatively good corrosion resistance at the macroscale with the exception of the Ni processed with N cold spray, as shown in Figure 19h & j. Further analysis on microscopic scale corrosion damage was performed in SEM.

A representative micrograph of the base material, interface, and cold spray regions for each sample type can be seen in Figure 20. In general, the base material (304L) exhibited small, hemispherical pits on the

order of 10–40 µm in diameter that were widely dispersed in their distribution. However, the Super C coated sample exhibited pits > 100 µm in diameter in the base material (Figure 20p). Damage in the cold spray region is hard to discern as surface roughness and possible contamination remnants from processing limit the ability to identify pitting or localized corrosion. However, as seen previously with the optical images, the Ni N processed cold spray regions did exhibit obvious signs of corrosion (Figure 20o). Finally, the interface regions, through SEM, were further observed to be the areas of largest concern. In general, for blended interfaces, higher densities of pitting occurred in the interface regions, often next to or underneath cold spray particles where the particles are present but do not form a fully dense layer (Figure 20b,e,k,&q). In the case of the Nickel N sample, the pitting corrosion is so severe that it has agglomerated into one large band of pits and no remaining cold spray particles exist in the interface region (Figure 20k). For the masked interfaces, a dual-mode of corrosion appears to be present. Crevicing occurs at the base of the mask, potentially undercutting the CS coating (Figure 20h & n). Additionally, in both CS coating cases, an enhanced band of pitting corrosion occurs roughly 500 micrometers away from the interface itself. This band is likely present due to the establishment of a galvanic couple, but the distance to the interface may be influenced by the underlying residual stresses and/or potential changes in near-surface microstructure.

Base Material	**Interface**	**Cold Spray**
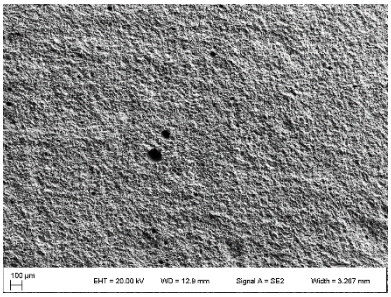	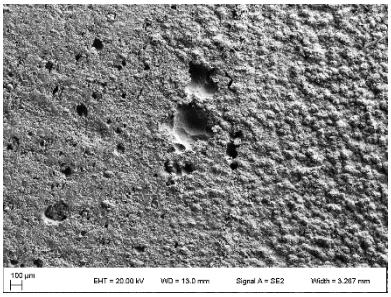	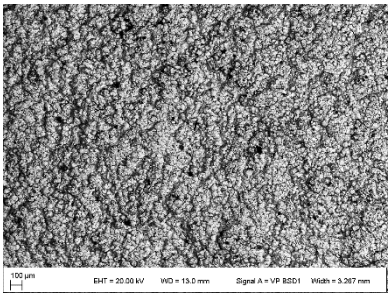
a) SS 304/304L substrate left of interface	b) Inconel processed with He blended interface	c) Inconel processed with He right of interface
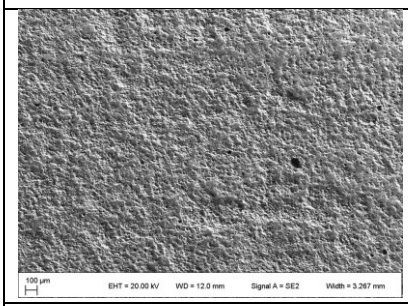	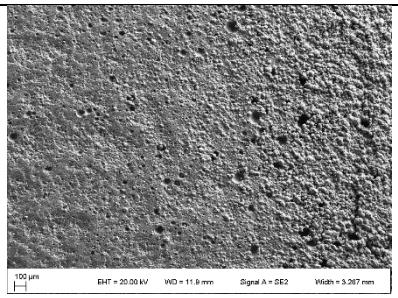	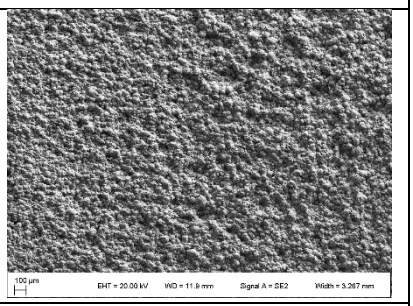
d) SS 304/304L substrate left of interface	e) Inconel processed with N blended interface	f) Inconel processed with N right of interface
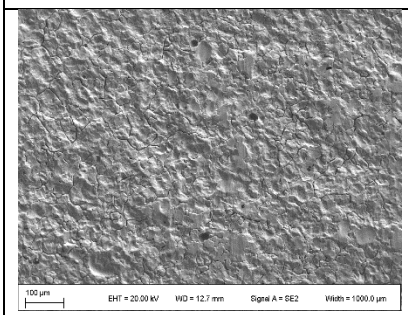	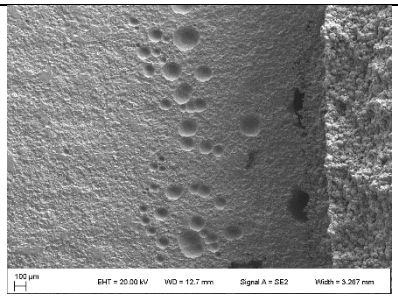	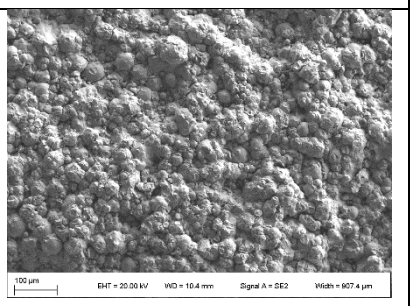

g) SS 304/304L substrate left of interface	h) Inconel processed with N masked interface	i) Inconel processed with N right of interface

Figure 20. First set of SEM secondary electron images of the base material, interface, and cold spray regions of the samples post 72 h exposure in $FeCl_3$ solution at 22 °C for a)–c) Inconel processed with He, d)–f) Inconel processed with N, g)–i) Inconel processed with N and masked. Samples are all oriented in the same direction with base material on the left and cold spray on the right of the images. Image letters continue in next figure.

Base Material	Interface	Cold Spray
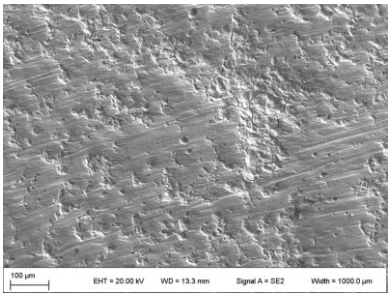	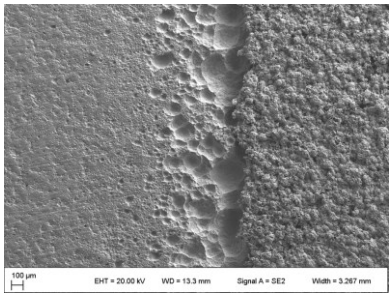	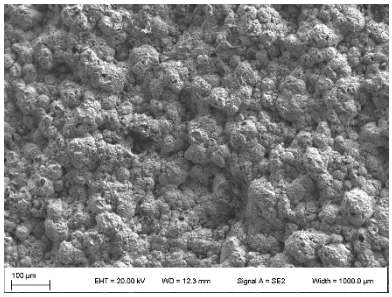
j) SS 304/304L substrate left of interface	k) Super C processed with N blended interface	l) Super C processed with N right of interface
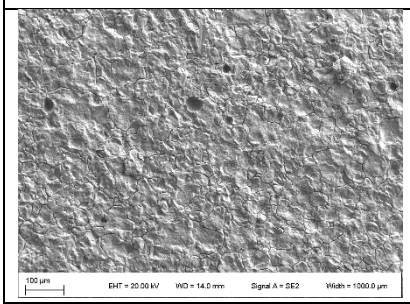	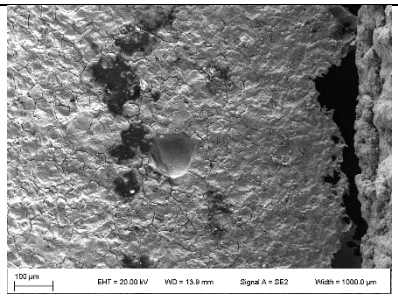	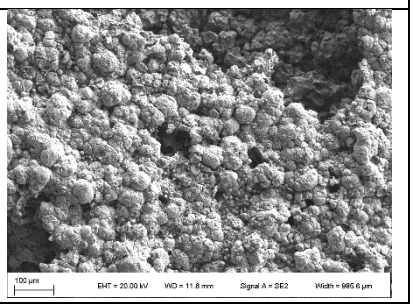
m)SS 304/304L substrate left of interface	n) Ni processed with N masked interface	o) Ni processed with N right of interface
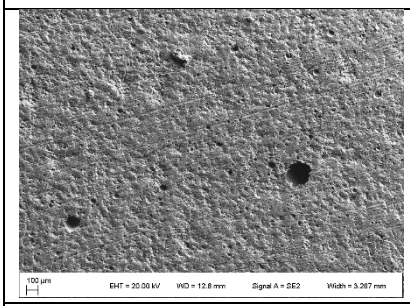	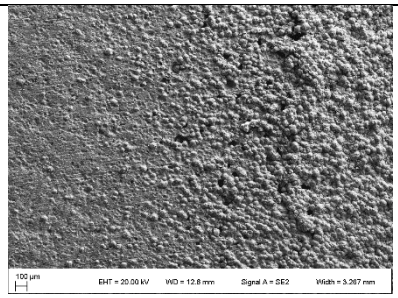	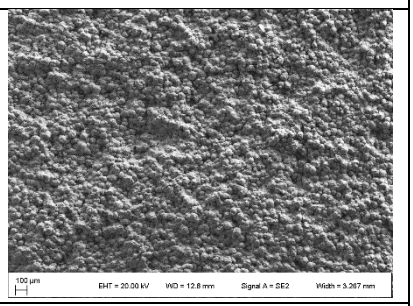
p) SS 304/304L substrate left of interface	q) Super C processed with N SS blended interface	r) Super C processed with N right of interface

Figure 21. Second set of SEM secondary electron images of the base material, interface, and cold spray regions of the samples post 72 h exposure in $FeCl_3$ solution at 22 °C for j)–l) Ni processed with N, m)–o) Ni processed with N and masked, and p)–r) Super C processed

with N. Samples are all oriented in the same direction with base material on the left and cold spray on the right of the images. Image letters continued from previous figure.

In addition to SEM analysis, EDS was performed to identify any larger scale potential contamination due to processing that might lead to the localized corrosion damage. Examples of EDS analysis for the Ni CS processed with nitrogen for the blended and masked sample interfaces are shown in Figure 22. No apparent contamination could be correlated with areas of enhanced corrosion damage, and therefore, corrosion is likely governed by other factors, such as the galvanic potential between the CS and base material, potential residual stresses, surface roughness, and/or microstructural changes due to the CS coatings.

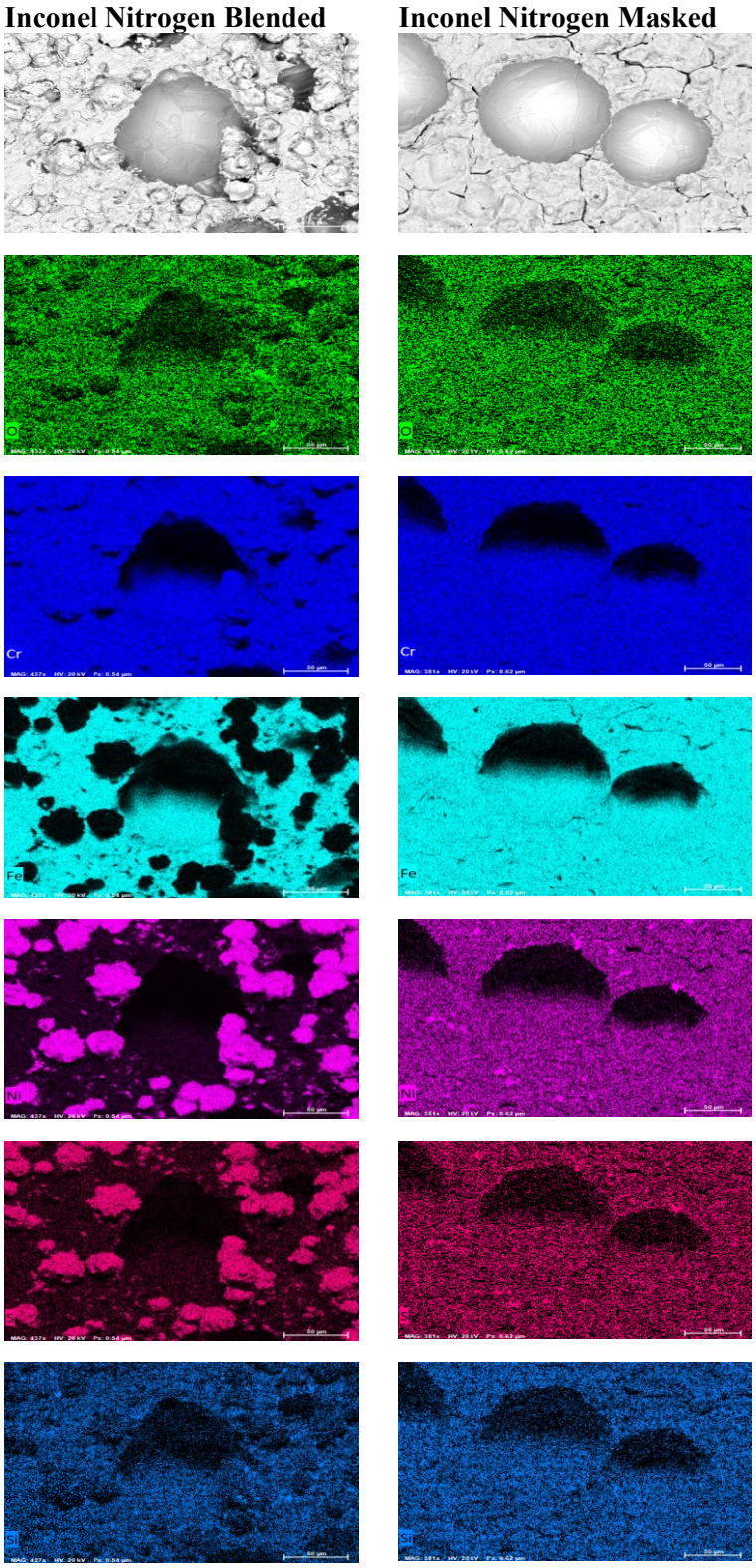

Figure 22. Example SEM and corresponding EDS of the interface regions of the Ni cold spray processed with nitrogen for the blended (left) and masked (right) interfaces.

2.5 Implications and Future Work

From the full immersion accelerated electrochemical testing, it is evident that the surface roughness of the cold spray material plays a role in its susceptibility to metastable pitting. Grinding samples greatly reduced the presence of metastable pit indications across all samples. Additionally, in comparison to the base material, while most materials selected were chosen for their better compatibility with SS, they still all display a significantly different OCP than the base material, suggesting that galvanic corrosion could be a potential issue for the cold spray/base material interface.

From exposure in $FeCl_3$ accelerated pitting testing, it is evident that all interfaces of the samples tested presented the most deleterious regions for pitting to occur. In blended samples, pitting was exacerbated under regions of not fully dense particles of cold spray. In the masked samples, two modes of corrosion were observed: crevice at the connection between the base material and cold spray, and enhanced pitting zones in the near interface regions. Further study is necessary to fully understand the mechanisms behind the enhanced corrosion attack. Future plans include cross-sectioning these pre-exposed samples to determine the full extent of corrosion attack and potential relationship to microstructural changes and/or changes in residual stress. Additionally, full immersion $FeCl_3$ pitting testing will be carried out on ground CS coated samples (cut from the same plates/specimens as those tested here) to examine the influence of surface roughness on the corrosion occurring at the interface. Finally, an expanded set of CS materials and processing conditions will be examined in the coming year to identify enhancements to corrosion resistance.

3 FY22 Work

Prior to fabricating test coupons, preparatory work was done to ensure meaningful data will be generated.

3.1 Criteria for Comparative Analysis of CISCC Performance

High-fidelity CISCC analysis and testing is cost- and time-prohibitive for down selection of top-performing processes and parameters. Therefore, accelerated corrosion testing, such as ASTM G36 and ASTM G61-86 (ASTM G61-86(2018)), are to be conducted to benchmark the corrosion resistance of each material. Learnings from this testing will generate understanding of how process parameters affect microstructure and CISCC resistance and will inform additional processes and material system optimization work at PNNL.

This section discusses criteria required for comparative analysis of CISCC performance. For comparative CISCC analysis of cold spray chemistries and developed microstructures, test methods must (1) normalize surface geometry, (2) account for residual stresses, (3) be in a controlled and appropriate test environment, and (4) be numerically quantifiable and repeatable. Failure to meet these criteria could result in outcomes that cannot be used for comparative analysis of processes and materials.

Once cold spray chemistries are optimized, surface geometry effects can be investigated. Powder processing, surface preparation and process parameters affect cold spray surface geometry. Effects of these parameters on surface geometry and CISCC performance is an important undertaking. Additionally, it is important to quantify CISCC performance of post processed cold sprayed materials. Layers of cold sprayed material are strengthened by additional deformation and compaction caused by the impact of several subsequent layers of cold spray. Properties are homogeneous throughout the depth of a cold spray coating except for the outermost layers which are typically removed by post processes, such as buffing, grinding, or machining. Test methods for comparing surface geometry effects must (1) account for

residual stresses, (2) be in a controlled and appropriate test environment, and (3) be numerically quantifiable and repeatable. Failure to meet these criteria could result in outcomes that cannot be used for comparative analysis of processes and materials. These criteria can also be used for comparative benchmarking of materials and processes as they would exist in the field or process optimization after a material system has been selected. CISCC performance is a compound of chemistry, microstructure, and surface finish. It may not be possible to decouple the effects of these factors unless prior testing was done with normalized surface geometries.

Learnings from the accelerated corrosion testing and process optimization will be used to down select top-performing processes for detailed analysis and testing. Top-performing processes will be applied to coupons fabricated from a single heat of SS 304/304L. These coupons will be tested in four-point bending systems designed for CISCC testing at PNNL using direct current potential drop to perform in situ monitoring of crack formation and growth.

In addition, cold spray should be performed over arc welded test samples with and without laboratory generated CISCC cracks in the welds to simulate mitigating field repair conditions for CISCC. Arc welded specimens without application of cold spray should also be tested as control samples. This will allow evaluation of the effectiveness of cold spray in mitigating both CISCC initiation and growth.

3.1.1 Surface Geometry and Post Processing

Surface finish strongly affects CISCC. For new fabrication, repair, or mitigation of canisters, welds are ground or machined flush. Many studies (Ghosh and Kain 2010; Turnbull et al. 2011; Acharyya et al. 2012; Lyon et al. 2015; Zhou et al. 2016; Mankari and Acharyya 2017) have shown that machining or grinding of austenitic SS generally strongly affects CISCC resistance, as determined by ASTM G36. Several works (Turnbull et al. 2011; Lyon et al. 2015) noted that pitting and cracks *first formed along machining grooves and other surface disruptions*. This means that for the conditions reviewed in these studies, the surface condition appeared to be a leading factor for reduced CISCC resistance. Specifically, it is reported that a very smoothly machined surface or ground surface featuring a thin work-hardened layer with presence of micro-cracks and grain fragmentation can adversely affect CISCC resistance. It is important to note that mechanical polishing produces a nanocrystalline layer at the surface that is reported to be very corrosion-resistant and different from the original material (Wang et al. 2015). Therefore, processes such as electropolishing should be considered comparative analysis of cold sprayed microstructure with normalized surface topology is desired. FY 22 work will focus on analyzing as sprayed and field capable post processing techniques.

In one study (Mankari and Acharyya 2017), sanding was followed by buffing. This process produced a surface with reduced plastic strain, reduced surface roughness, and induced compressive residual stresses at the surface. ASTM G36 testing showed that this process significantly improved CISCC resistance relative to other conditions evaluated. These studies show that final surface processing can have a strong effect on CISCC initiation.

Arc welded and cold sprayed components are typically machined or ground after processing across all industries. For new fabrication, repair, or mitigation of canisters, it could be assumed that processed regions will be machined or ground. Based on the literature and understanding of relevant physics discussed in this section, it is reasonable to include a final material removal step, such as buffing, lapping, or polishing after the weld is ground or machined flush.

As far as the authors are aware, regarding cold spraying for nearly all applications, the top ~0.5 mm of the surface is removed. This is because it takes multiple layers of cold spray to fully densify material underneath. Even for cold spraying, it is important to normalize the surface by polishing to remove the transitory microstructure that exists in the top ~200 μm. However, for repairs within an overpack, removal of this top layer may be impractical and unnecessary. If needed, addition of a material removal process to stationary cold spray systems or robotic crawlers is doable. It is important to establish an

understanding of cold spray surface effects on CISCC resistance. Surface roughness of cold spray coatings is dependent on spray conditions and post processing, such as grinding, machining, or buffing. Work done in FY22 will enhance understanding of surface roughness effects and determine if post processes are needed.

3.2 Continued Process Development and Exploratory Testing

Based on learnings from the FY21 work, cold spray conditions, material systems, and process parameters will be explored and optimized through iterative experimentation and analysis. Based on current results, increasing effort will be put to reducing the potential for galvanic effects through cold spray powder composition selection, testing ground and/or buffed cold sprayed deposits, and working to further understand corrosion at the exposed coating/substate interface. These are important topics that need to be understood to inform decision making relative to powder chemistry and post processing.

3.3 ASTM G36 with Additional Controls

ASTM G36 is an accelerated test method of ranking the CISCC susceptibility for SS and related alloys. The materials being tested are immersed in a boiling magnesium chloride solution and are monitored periodically for examination of crack initiation. The aggressive nature of the boiling magnesium chloride expedites CISCC in materials, making it an effective method to quickly screen among a variety of materials. This test method is ideal for identifying the effects of composition, heat treatment, surface finish, microstructure, and stress on the CISCC susceptibility of materials.

ASTM G36 allows for a great deal of flexibility relative to how components are tested. To ensure repeatability and the criteria for comparative analysis, established in the previous section, are met, the following procedures are added:

1. Coupons will be placed into four-point bend fixtures such that tensile residual stresses, representative of those produced by fabrication welds, exist on the exposed surface of the coupon.
2. Cold spray coating will be generated using varying processing parameters and deposited onto the convex face of the coupons after they are placed into bending.
3. Prior to testing, the surface roughness of the side of the coupons that have been cold sprayed will be measured.
4. An accelerated screening test following the ASTM G36 standard will be performed on all coupons.
5. Coupons will be removed and inspected periodically. Time to first observed crack and total crack length at time intervals will be recorded. This will provide quantifiable test results that can be directly used to guide parametric optimization.

This testing will be used to enhance understanding of surface finish, exposed coat/substrate effects, and potential galvanic concerns. This testing will be used to competitively benchmark cold spray processes to inform down selection for further study. Testing this year will include evaluation of the interface between the cold spayed coating and the substrate and the effect of post processes, such as grinding and buffing.

3.4 Cold Spray Technology Development Roadmap

Technical road mapping activities will begin with establishing priorities and associated target specifications. Defining the relative importance of types of cold spray applications is important because they have competing system configurations and objectives.

Nozzle clogging is an issue in portable HPCS systems when spraying Ni and Ni-based alloys. Clogging can be solved by developing cooled nozzles for portable systems or adding hard particles, such as

carbides, to the powder. Hard particles can improve the mechanical properties of the deposited material but could cause localized galvanic effects that accelerate pit formation. Nozzle cooling and the effects of hard particles are areas that need to be investigated for applications using portable equipment.

A significant amount of work needs to be done to develop HPCS for DCSS canister repair and mitigation. Coating powder chemistries need to be selected such that no detrimental galvanic effects occur and CISCC resistance is maximized. Identifying the optimal chemistry for canister protection is an area that demands a significant R&D effort.

Surface roughness/texture effects are expected to affect CISCC initiation. Cold spray parameters and powder preparation can affect surface roughness. Testing should be done to develop an understanding of how surface roughness/texture developed by cold spray affects CISCC initiation.

Edge effects and interfaces between the coatings and substrates exposed to the environment need to be investigated. For example, deposited coatings could produce geometric discontinuities that enable crevice corrosion. If this is the case, a groove and blend technique (Figure 23 bottom) can be used to normalize surface geometry. Alternatively, grinding or buffing edges of a deposited costing without a groove could be a solution.

Cold spray done within an overpack is challenging due to space confinements. For cold spray in confined spaces, portable cold spray systems, which have remote gas heating, and angled nozzles are used. Remote gas heating limits spray gas temperature. Velocity reduction and associated angled nozzles require expensive helium gas to be used for all materials of interest for canister life extension. Velocity reduction and flow direction change dramatically reduce deposition efficiency to below 50% for materials that can be sprayed with stationary equipment at greater than 99.9% efficiency. Angled nozzles and lack of nozzle cooling cause nozzle clogging to occur quickly in portable systems. These issues are specific to cold spray in confined spaces that only apply to repairs within the overpack. Overcoming issues associated with angled nozzle spraying in a confined space is an important undertaking for development of repair within the overpack.

For all other cold spray operations, factory type equipment using straight nozzles and improved heating can produce high-quality coatings at a fraction of the cost per unit weight of deposited materials if developed correctly. Nozzle cooling, higher gas temperatures, and helium recycling provide process advantages and improved economics. Developing processes that leverage these advantages can enable favorable economics for coating entire canisters, or large areas of canisters, as part of DOE acceptance of canisters. Cost~~s~~ reduction is also of interest for application of cold spray over arc welds and HAZs as part of new canister fabrication.

Road mapping activities will ensure that cold spray development activities optimize value to stakeholders and reflect Spent Fuel and Waste Disposition priorities despite the divergence of technical challenges between cold spray applications. Material system optimization, surface preparation, and other technical challenges being addressed in the current work scope apply to all cold spray applications for canister life extension. Structural and mechanical requirements need to be evaluated for thorough evaluation of the cold spray technology for this application. For example, does the coating need to survive being dragged across rails or scraping against concrete while being lowered into the overpack? If so, what are the laboratory test metrics that prove the coating can meet these needs? It is important to understand that coatings and base metals react loads together, not independently. Structural analysis, using FEA, and mechanical testing will likely be needed to understand the combined behavior of the coating and canister base metal. This understanding can inform coating property requirements.

Figure 23. Coating strategies for localized coatings. Top: deposited coating without groove or blend. Bottom: grooved and blended coating.

Process optimization to develop optimal nozzle design, surface preparation, powder preparation, and quality control/assurance techniques are needed after coating chemistry is finalized and geometric effects are understood.

This page is intentionally left blank

4 REFERENCES

Acharyya SG, A Khandelwal, V Kain, A Kumar and I Samajdar. 2012. "Surface working of 304L stainless steel: Impact on microstructure, electrochemical behavior and SCC resistance." *Materials Characterization* 72:68-76. DOI: https://doi.org/10.1016/j.matchar.2012.07.008.

Alidokht SA, P Manimunda, P Vo, S Yue and R Chromik. 2016. "Cold spray deposition of a Ni-WC composite coating and its dry sliding wear behavior." *Surface & Coatings Technology* 308:424-434.

Alloys R. 2020. "Stress Corrosion Cracking." Rolled Alloys. Accessed 07/18/2020, 2020. Available at https://www.rolledalloys.com/technical-resources/blog/stress-corrosion-cracking.

Archard JF. 1953. "Contact and Rubbing of Flat Surfaces." *Journal of Applied Physics* 24(8):981-988. DOI: 10.1063/1.1721448.

ASTM G133-05(2016). 2016. "Standard Test Method for Linearly Reciprocating Ball-on-Flat Sliding Wear." *A International*, West Conshohocken, PA: 10.1520/G0133-05R16. Available at http://www.astm.org/cgi-bin/resolver.cgi?G133-05(2016).

ASTM G61-86(2018). 2018. "Standard Test Method for Conducting Cyclic Potentiodynamic Polarization Measurements for Localized Corrosion Susceptibility of Iron-, Nickel-, or Cobalt-Based Alloys." West Conshohocken, PA: ASTM International. DOI: 10.1520/G0061-86R18. Available at http://www.astm.org/cgi-bin/resolver.cgi?G61.

Champagne V. 2018. *Cold Spray Action Team Meeting*. https://55922c16-bbf4-4650-aa4d-6d5bfb8c7a14.filesusr.com/ugd/0c16db_6033445adae64430944290915af890a5.pdf.

2014. "Standard Test Methods for Determining Area Percentage Porosity in Thermal Sprayed Coatings." *A International*, West Conshohocken, PA:10.1520/E2109-01R14. Available at http://www.astm.org/cgi-bin/resolver.cgi?E2109-01(2014).

Fiebig J, E Bakan, T Kalfhaus, G Mauer, O Guillon and R Vaßen. 2020. "Thermal Spray Processes for the Repair of Gas Turbine Components." *Advanced Engineering Materials* 22(6):1901237. DOI: 10.1002/adem.201901237.

Ghosh S and V Kain. 2010. "Effect of surface machining and cold working on the ambient temperature chloride stress corrosion cracking susceptibility of AISI 304L stainless steel." *Materials Science and Engineering: A* 527(3):679-683. DOI: https://doi.org/10.1016/j.msea.2009.08.039.

Glass SW, MR Larche, MS Prowant, JD Suter, JP Lareau, X Jiang and KA Ross. 2018. "Cold spray NDE for porosity and other process anomalies." *AIP Conference Proceedings* 1949(1):020010. DOI: 10.1063/1.5031507.

Günen A, E Kanca, H Çakir, MS Karakaş, MS Gök, Y Küçük and M Demir. 2017. "Effect of borotitanizing on microstructure and wear behavior of Inconel 625." *Surface and Coatings Technology* 311:374-382. DOI: https://doi.org/10.1016/j.surfcoat.2016.12.097.

Hanson B, H Alsaed, C Stockman, D Enos, R Meyer and K Sorenson. 2012. *Gap Analysis to Support Extended Storage of Used Nuclear Fuel, Rev. 0*. FCRD-USED-2011-000136 Rev. 0; PNNL-20509. Washington, D.C.: U.S. Department of Energy. Available at https://www.osti.gov/servlets/purl/1133836.

Haynes. 2020. "Resistance to Stress Corrosion Cracking." Haynes International. Accessed 07/18/2020, 2020. Available at http://www.haynesintl.com/alloys/alloy-portfolio_/Corrosion-resistant-Alloys/HASTELLOY-C-276-Alloy/resistance-to-stress-corrosion-cracking.

Hosler R and J Hall. 2010. *Outside Diameter Initiated Stress Corrosion Cracking*. PWR Owners Group. Available at https://www.nrc.gov/docs/ML1104/ML110400241.pdf.

Howe C. 2017. *Economics of Helium Recovery for Cold Spray*. Cold Spray Action Team Workshop 2018. Available at http://www.coldsprayteam.com/Howe_2017%20CSAT%20-%20Chris%20Howe%20-%20Moog.pdf.

Lareau JP. 2014. "Operating Experience with Chloride Induced Stress Corrosion Cracking " In *EPRI ESCP*, Charlotte, NC.

Lareau JP, A Parsi, B Gabriel and V Champagne. 2012. "Cold Spray Coatings for Prevention and Mitigation of Stress Corrosion Cracking." In *Cold Spray Action Team Meeting*, Worcester, MA.

Available at https://55922c16-bbf4-4650-aa4d-6d5bfb8c7a14.filesusr.com/ugd/0ebd9c_ba228f5af07c41149076c2fb1e50af43.pdf.
Luo X-T, M-L Yao, N Ma, M Takahashi and C-J Li. 2018. "Deposition behavior, microstructure and mechanical properties of an in-situ micro-forging assisted cold spray enabled additively manufactured Inconel 718 alloy." *Materials & Design* 155:384-395. DOI: https://doi.org/10.1016/j.matdes.2018.06.024.
Lyon KN, TJ Marrow and SB Lyon. 2015. "Influence of milling on the development of stress corrosion cracks in austenitic stainless steel." *Journal of Materials Processing Technology* 218:32-37. DOI: https://doi.org/10.1016/j.jmatprotec.2014.11.038.
Mankari K and SG Acharyya. 2017. "Development of stress corrosion cracking resistant welds of 321 stainless steel by simple surface engineering." *Applied Surface Science* 426:944-950. DOI: https://doi.org/10.1016/j.apsusc.2017.07.223.
Moridi A, SM Hassani-Gangaraj, M Guagliano and M Dao. 2014. "Cold spray coating: review of material systems and future perspectives." *Surface Engineering* 30(6):369-395. DOI: 10.1179/1743294414Y.0000000270.
Nardi A, V Champagne, G Ferguson, I Nault, W Story and D Nikolov. 2019. "Chrome Replacement and Recent Advancements." In *Cold Spray Action Team Meeting*. Available at https://55922c16-bbf4-4650-aa4d-6d5bfb8c7a14.filesusr.com/ugd/0ebd9c_638d644acea54db3b7695142978f938a.pdf.
NRC. 2012. *Potential Chloride-Induced Stress Corrosion Cracking of Austenitic Stainless Steel and Maintenance of Dry Cask Storage System Canisters*. NRC Information Notice 2012-20. Washington, DC: U.S. Nuclear Regulatory Commission. Available at http://www.nrc.gov/docs/ML1231/ML12319A440.pdf. ADAMS Accession No. ML12319A440.
Ross KA, X Jiang, M Alabi and CW Enderlin. 2020. *Investigation of Cold Spray as a Dry Storage Canister Repair and Mitigation Tool*. ; Pacific Northwest National Lab. (PNNL), Richland, WA (United States). (PACIFIC NW LAB)
(ORCID:0000000224620680)
[BATTELLE]. Available at https://www.osti.gov/servlets/purl/1765140.
Ross KA, JP Lareau, SW Glass and RM Meyer. 2021. *Assessment of Cold Spray Technology for Nuclear Power Applications*. Washington, D.C.: U.S. Nuclear Regulatory Commission. Available at https://adamswebsearch2.nrc.gov/webSearch2/main.jsp?AccessionNumber=ML21263A107. ADAMS Accession No. Adams Accession No. ML21263A107.
Schneider CA, WS Rasband and KW Eliceiri. 2012. "NIH Image to ImageJ: 25 years of image analysis." *Nature Methods* 9(7):671-675. DOI: 10.1038/nmeth.2089.
Torgerson T, MD Harris, S Alidokht, TW Scharf, S Aouadi, R Chromik, J Zabinski and A Voevodin. 2018. "Room and elevated temperature sliding wear behavior of cold sprayed Ni-WC composite coatings." *Surface and Coatings Technology* 350. DOI: 10.1016/j.surfcoat.2018.05.090.
Turnbull A, K Mingard, JD Lord, B Roebuck, DR Tice, KJ Mottershead, ND Fairweather and AK Bradbury. 2011. "Sensitivity of stress corrosion cracking of stainless steel to surface machining and grinding procedure." *Corrosion Science* 53(10):3398-3415. DOI: https://doi.org/10.1016/j.corsci.2011.06.020.
TWI. 2020. "What is Thermal Spraying?" The Welding Institute. Accessed 07/08/2020, 2020. Available at https://www.twi-global.com/technical-knowledge/faqs/faq-what-is-thermal-spraying.
VRC. 2020. "Cold Spray vs Thermal Spray – An Overview." VRC Metal Systems. Accessed 07/18/2020, 2020. Available at https://www.vrcmetalsystems.com/blog-post/cold-spray-vs-thermal-spray/.
Wang Z, Y Yan and L Qiao. 2015. "Tribocorrosion Behavior of Nanocrystalline Metals — a Review." *Materials transactions* 56(11):1759-1763. DOI: 10.2320/matertrans.M2015280.
Yeom H, T Dabney, N Pocquette, K Ross, FE Pfefferkorn and K Sridharan. 2020. "Cold spray deposition of 304L stainless steel to mitigate chloride-induced stress corrosion cracking in canisters for used nuclear fuel storage." *Journal of Nuclear Materials* 538:152254. DOI: https://doi.org/10.1016/j.jnucmat.2020.152254.

Zhou N, R Pettersson, R Lin Peng and M Schönning. 2016. "Effect of surface grinding on chloride induced SCC of 304L." *Materials Science and Engineering: A* 658:50-59. DOI: https://doi.org/10.1016/j.msea.2016.01.078.

This page is intentionally left blank

Appendix A